Thermodynamics of strong interactions

V. I. Yukalov and E. P. Yukalova
Joint Institute for Nuclear Research, Dubna, Russia; Queen's University, Kingston, Canada

Fiz. Élem. Chastits At. Yadra **28**, 89–161 (January–February 1997)

The state of the art in studying thermodynamic properties of hot and dense nuclear matter is reviewed with special emphasis on the confinement–deconfinement transition between hadron matter and quark–gluon plasma. The most popular models used for describing deconfinement are analyzed, including statistical bootstrap models, pure phase models, the model of clustered quarks, and the string-flip potential model. Predictions of these models are compared with lattice numerical simulations. It is concluded that precursor fluctuation effects must be taken into account in order to get a realistic description of the deconfinement transition. The existence of precursor fluctuations is in line with the dynamical confinement scenario and suggests that deconfinement cannot be considered as a transition between pure hadron and quark–gluon phases. All this supports the concept of cluster coexistence advocated by the authors of this review: Quark–gluon plasma and hadron clusters are different quantum states of the same system, so that any statistical model pretending to treat nuclear matter under extreme conditions must incorporate the probability of these different channels. The ways of constructing statistical models with plasma–cluster coexistence are discussed, and thermodynamic properties of such models are analyzed. [S1063-7796(97)00301-X]

1. INTRODUCTION

One of the most intriguing problems of high-energy physics is the possibility of transforming the nuclear matter composed of hadrons into the phase consisting of their fundamental constituents, quarks and gluons. This phase, because of the apparent analogy with the electron–ion plasma, is called the quark–gluon plasma. The transformation of the hadron matter into the quark–gluon plasma is called deconfinement; the inverse process is called confinement. The deconfinement transition is somewhat similar to the ionization of atoms. The literature devoted to this phenomenon is so voluminous that, to avoid overloading the list of references, we shall cite here mainly review papers when these are available, in which the reader can find thousands of references to original works. The specific feature of the present review is that we concentrate on the statistical models of strongly interacting systems under extreme conditions, when nonhadronic degrees of freedom become important and deconfinement occurs.

The possibility that quark degrees of freedom can come into play in the process of relativistic nuclear collisions at already achieved accelerator energies was advanced by Baldin,[1] who predicted and explained the cumulative effect as a manifestation of the formation in the colliding nuclei of multiquark droplets.

In order that quark–gluon degrees of freedom be essential, special conditions are necessary, like high temperature or density. From quantum chromodynamics it is known that at asymptotically high temperature quarks and gluons are really deconfined, forming the quark–gluon plasma.[2–6] We also know that at zero temperature and at the normal density of nuclear matter there is complete confinement, so that only hadrons exist. But where is the intermediate region in which quark–gluon degrees of freedom become relevant? The characteristic parameters for this region can be estimated as follows.

Nuclear matter in the normal state has the baryon density $n_{0B}=0.167/\text{fm}^3$. The corresponding normal quark density is $\rho_0\equiv 3n_{0B}=0.5/\text{fm}^3$. The characteristic quark interaction energy in the normal state can be represented as $E_0=\hbar/\tau_0$, with the interaction time $\tau_0=a_0/c$, where $a_0=\rho_0^{-1/3}$ is the mean interquark distance in the normal state. Adopting the system of units in which $\hbar=c=1$, with the conversion constant $\hbar c=197.327$ MeV·fm, we have

$$E_0=\rho_0^{1/3}=157 \text{ MeV}.$$

We note an interesting relation between this interaction energy and the characteristic baryon energy density, $\varepsilon_B\equiv m_N n_{0B}$, in which $m_N\equiv\frac{1}{2}(m_p+m_n)=939$ MeV is the average nucleon mass. Since $\varepsilon_B=157$ MeV/fm^3, we have $E_0=\varepsilon_B$ fm^3. Thus, the normal nuclear matter should start to decompose on being heated up to the temperature equal to the quark interaction energy E_0, that is, up to $\Theta_c\approx 160$ MeV.

If one wishes to destroy the hadron matter by compression, one has to reach a density of about the density of quarks inside a nucleon. This characteristic density is $\rho_c\equiv 3/v_N$, where $v_N\equiv(4\pi/3)r_N^3$ is the nucleon volume. Taking for the nucleon radius $r_N=0.9$ fm, we get $v_N=3$ fm^3. From this,

$$\rho_c=2\rho_0=1/\text{fm}^3.$$

This tells us that the hadron matter should start disintegrating on being compressed up to the density $\rho_c\approx 2\rho_0$.

As we see, the expected critical temperature and density are fairly low. Such conditions certainly existed in the early Universe about 10^{-5}–10^{-4} sec after the Big Bang and are likely to exist in the interior of neutron stars.[7]

More important is the common belief that such conditions can be created in the process of relativistic heavy-ion collisions, even with existing accelerators, thus opening the

path for experimental observation of the quark–gluon plasma in the laboratory.[8–14] Analogous relativistic nuclear collisions can also be studied in cosmic-ray experiments.[8] The density of matter inside a fireball formed by two colliding ions can reach $10\rho_0$.

All models of the formation of the quark–gluon plasma in nuclear collisions require information about its rate of thermalization. Does the matter inside a fireball thermalize sufficiently fast, so that a thermodynamic description makes sense? For this, the thermalization time must be shorter than the fireball lifetime $\tau_f \sim 10^{-22}$ sec. The thermalization time, or the time of local equilibration, τ_{loc}, can be estimated as follows.[13–15] The local equilibrium time is $\tau_{\text{loc}}=\lambda/c$, in which $\lambda=(\rho\sigma)^{-1}$ is the mean free path of a particle in the medium, $\rho=a^{-3}$ is the density of matter, a is the average interparticle distance, $\sigma\sim b^2$ is the cross section, and b is the interaction radius. Adopting the values $a\sim b\sim 1$ fm typical of nuclear matter, we have $\lambda\sim 1$ fm and $\tau_{\text{loc}}\sim 10^{-23}$ sec. Because of the inequality $\tau_{\text{loc}}\ll\tau_f$, the thermalization inside a fireball is likely to be reached.

The possibility of speaking about the thermodynamics of strong interactions, separately from electromagnetic and weak interactions, is based on the fact that it is just this type of interaction which in many cases plays the dominant role. In fact, the dimensionless coupling constant of strong interactions, $\alpha_s\approx 1$, is much larger than the coupling constants of electromagnetic interactions, $\alpha_e\approx 1/137\sim 10^{-2}$, and of weak interactions, $\alpha_w\sim 10^{-5}$, to say nothing of the coupling constant of gravitational interactions, $\alpha_g\sim 10^{-12}$. The corresponding interaction times, at the energy 1 GeV characteristic of high-energy physics, are $\tau_s\sim 10^{-24}$ sec for strong interactions, $\tau_e\sim 10^{-21}$ sec for electromagnetic interactions, and $\tau_w\sim 10^{-10}$ sec for weak interactions. Therefore, during the lifetime of a fireball, $\tau_f\sim 10^{-22}$ sec, electromagnetic and weak interactions do not play any role. In the interval of time $\tau_{\text{loc}}<t<\tau_f$ inside a fireball there may exist an equilibrium state of strongly interacting particles.

The only consistent way of calculating thermodynamic characteristics in quantum chromodynamics is perturbation theory, which is quite similar to that of quantum electrodynamics.[16,17] However, the effective coupling parameter of strong interactions becomes small only at asymptotically high temperatures. In the most interesting region of temperatures around $\Theta_c\approx 160$ MeV, where deconfinement occurs, the coupling parameter is large and perturbation theory does not work. For describing the whole range of thermodynamic variables, several statistical models have been suggested.

2. STATISTICAL BOOTSTRAP MODELS

The usefulness of applying statistical methods for considering heated and compressed nuclear matter has been understood a long time ago. Let us mention, e.g., Fermi.[18]

The first statistical model of nuclear matter under extreme conditions, such as those realized inside fireballs, was proposed by Hagedorn[19] (see also Ref. 20) and is called the statistical bootstrap model. In this approach it is assumed that, at zero baryon density $n_B=0$, various hadrons can be generated from the vacuum with the mass distribution

$$\rho(m)=\rho_{\text{dis}}(m)+\rho_{\text{con}}(m); \quad m\in[0,\infty),$$

in which the first and second terms correspond to discrete and continuous mass spectra, respectively:

$$\rho_{\text{dis}}(m)=\sum_i \zeta_i\delta(m-m_i)[1-\Theta(m-m_0)],$$

$$\rho_{\text{con}}(m)=\Theta(m-m_0)\frac{a_0}{m^{5/2}}\exp\left(\frac{m}{\Theta_0}\right),$$

where $\Theta(\cdot)$ is the unit step function; ζ_i is a degeneracy number for spin–isospin states; and the parameters are

$$m_0=1000 \text{ MeV}, \quad a_0=6.5\times 10^3 \text{ MeV}^{3/2},$$

$$\Theta_0=160 \text{ MeV}.$$

The pressure for the ideal hadron gas is written in the classical Boltzmann approximation,

$$p=\Theta\int\rho(m)\exp(-\beta\sqrt{k^2+m^2})\frac{d\mathbf{k}}{(2\pi)^3}\,dm,$$

where Θ is the temperature in energy units, and β is the inverse temperature, $\beta\Theta\equiv 1$.

As can be easily checked, the pressure in this model diverges for all $\Theta\geq\Theta_0$. From this it was concluded[19] that Θ_0 is the limiting temperature of the Universe. The concept of the existence of a maximal temperature of the Universe is, of course, quite artificial, and therefore another interpretation of this divergence of the pressure has been proposed,[20] treating Θ_0 as the deconfinement temperature.

After Collins and Perry,[21] the geometrical scenario of deconfinement became popular.[22] According to this, the increase of temperature or baryon density leads to an increasing number of hadrons. The latter are assumed to have finite volumes.[23] When the number of hadrons becomes so high that their close packing occurs, they fuse into one gigantic hadron occupying the whole system. The Hagedorn temperature Θ_0 is interpreted as the fusion temperature, and the gigantic hadron cluster is identified with the system in the quark–gluon plasma state. This geometric scenario is reminiscent of the percolation transition.[24]

Following the geometric interpretation, the bootstrap model was modified[20] by invoking the excluded-volume approximation. In this, one considers N particles having the volumes $v_1, v_2, \ldots, v_N$ and moving in the free volume

$$V_N\equiv V-\sum_{j=1}^{N} v_j,$$

where V is the total volume of the system. The pressure in the excluded-volume approximation becomes

$$p=\frac{\Theta}{V}\ln\left\{\sum_{N=1}^{\infty}\frac{1}{N!}\Theta(V_N)\left[V_N\int\rho(m)\right.\right.$$

$$\left.\left.\times\exp(-\beta\sqrt{k^2+m^2})\frac{d\mathbf{k}}{(2\pi)^3}\,dm\right]^N\right\},$$

where again the Boltzmann approximation is used. The mass distribution for the discrete spectrum is taken in the same form as above, and for the continuous spectrum it is slightly modified as

$$\rho_{\text{con}}(m)=\Theta(m-m_0)\,\frac{a_0}{m^{\alpha}}\exp\left(\frac{m}{\Theta_0}\right),$$

with $3/2<\alpha<7/2$. Now, the pressure is everywhere finite and positive, becoming zero at the same temperature $\Theta_d\approx\Theta_0$. The temperature Θ_d at which $p(\Theta_d)=0$ is interpreted as the temperature of hadron fusion into a gigantic cluster. However, the thermodynamics of the system at $\Theta\to\infty$ has nothing to do with that of the ideal quark–gluon plasma.

To overcome the latter deficiency of the model, it has been argued that allowance for hadron compression can save the situation. This can be done[25] by complicating the mass distribution, writing its continuous part as

$$\rho_{\text{con}}(m,v)=\Theta(m-b_0v-m_0)\Theta(v-v_0)a_0(m-b_0v)^{\alpha}v^{\gamma}\exp\left\{\frac{4}{3}\,(\sigma_0v)^{1/4}(m-b_0v)^{3/4}\right\},$$

which now contains seven fitting parameters: $m_0,a_0,\alpha,b_0,v_0,\gamma,\sigma_0$.

Now, in accordance with the geometrical scenario, the number of hadrons at low temperature $\Theta<\Theta_d$ is proportional to the free volume, and at high temperatures $\Theta\to\infty$ this number tends to one symbolizing the formation of a gigantic cluster. However, at the first-order transition temperature Θ_d the number of hadrons $N(\Theta_d,V)$ diverges for any finite volume V, which is unreasonable.

The bootstrap models, in addition to the arbitrariness in postulating the mass distribution, contain internal deficiencies leading to the existence of instabilities contradicting the necessary stability conditions for statistical systems.[26,27]

3. PURE PHASE MODELS

An obvious idea would be to follow the standard Gibbs prescription for considering phase transitions between two phases. Treating the deconfinement as such a phase transition, one assumes the existence of two types of pure phases. At low temperatures and baryon densities this is a pure hadron phase with features typical of normal nuclear matter,[28] and at high temperature or baryon density it is the quark–gluon phase described by perturbative QCD.[17] Let Ω_1 be the grand potential of the quark–gluon plasma, and Ω_2 be that of the hadron matter. According to the Gibbs rule, a phase transition occurs when $\Omega_1(\Theta,\mu_B)=\Omega_2(\Theta,\mu_B)$, where μ_B is the baryon chemical potential. This equality gives a transition line $\Theta_d=\Theta_d(\mu_B)$. Expressing here the baryon potential $\mu_B=\mu_B(n_B)$ in terms the of baryon density, we can write $\Theta_d=\Theta_d(n_B)$.

The possibility of using perturbation theory for the high-temperature quark–gluon plasma is based on the property of asymptotic freedom. According to this property, the running coupling constant

$$\alpha_s(q)\simeq\frac{6\pi}{(11N_c-2N_f)\ln(q/\Lambda)}\left[1-\frac{51\ln\ln(q/\Lambda)}{121\ln(q/\Lambda)}\right],$$

in which N_c and N_f are the numbers of quark colors and flavors, respectively, $\Lambda\approx200$ MeV is a scale parameter, and q is the momentum, tends to zero as $q\to\infty$. In the integral over momenta defining the grand potential, the main contribution when $\Theta\to\infty$ comes from $q\approx\Theta$. Hence, it is possible to obtain an expansion in powers of $\alpha_s(\Theta)\equiv g^2(\Theta)/4\pi$ with the effective coupling parameter

$$g^2(\Theta)\simeq\frac{24\pi^2}{(11N_c-2N_f)\ln(\Theta/\Lambda)}.$$

As a result of this expansion,[29] neglecting the quark masses, one has for the grand potential

$$\frac{\Omega_1}{V}=-A\Theta^4+B,$$

in which a nonperturbative term B is included and the notation

$$A\equiv A_0+A_2g^2+A_3g^3+A_4g^4\ln g$$

is used, where

$$A_0=\frac{\pi^2}{45}\left[N_c^2-1+\frac{7}{4}N_cN_f+15N_c\sum_f\frac{\mu_f^2}{2\pi^2\Theta^2}\left(1+\frac{\mu_f^2}{2\pi^2\Theta^2}\right)\right],$$

$$A_2=-\frac{N_c^2-1}{144}\left[N_c+\frac{5}{4}N_f+9\sum_f\frac{\mu_f^2}{2\pi^2\Theta^2}\left(1+\frac{\mu_f^2}{2\pi^2\Theta^2}\right)\right],$$

$$A_3=\frac{N_c^2-1}{12\pi}\left(\frac{1}{3}N_c+\frac{1}{6}N_f+\frac{1}{3}\sum_f\frac{\mu_f^2}{2\pi^2\Theta^2}\right)^{3/2},$$

$$A_4=\frac{N_c^2-1}{16\pi^2}N_c\left(\frac{1}{3}N_c+\frac{1}{6}N_f+\sum_f\frac{\mu_f^2}{2\pi^2\Theta^2}\right),$$

in which μ_f is the chemical potential of an f-flavor quark. Note that the term $O(g^6)$ cannot be calculated by perturbation theory because of unrenormalizable infrared divergences.

We take into account the fact that the number of quark colors is $N_c=3$ and consider for simplicity the case of zero baryon density, $n_B=0$, so that $\mu_f=0$. Then the pressure of the quark–gluon plasma is

$$p_1\equiv-\frac{\Omega_1}{V}=A\Theta^4-B,$$

where the expansion coefficients of A are

$$A_0=\frac{8\pi^2}{45}\left(1+\frac{21}{32}N_f\right),\quad A_2=-\frac{1}{6}\left(1+\frac{5}{12}N_f\right),$$

$$A_3=\frac{2}{3\pi}\left(1+\frac{1}{6}N_f\right)^{3/2},\quad A_4=\frac{3}{2\pi^2}\left(1+\frac{1}{6}N_f\right).$$

The low-temperature hadron phase is often modeled[4,7,30] by a gas of massless noninteracting pions, which for the grand potential yields

$$\frac{\Omega_2}{V}=-\frac{\pi^2}{30}\Theta^4.$$

The corresponding pressure is

$$p_2\equiv-\frac{\Omega_2}{V}=\frac{\pi^2}{30}\Theta^4.$$

Equating Ω_1 to Ω_2, or p_1 to p_2, one obtains the deconfinement temperature

$$\Theta_d=\gamma B^{1/4};\quad \gamma\equiv\left(A-\frac{\pi^2}{30}\right)^{-1/4}.$$

To check the phase-transition order, let us find the latent heat at the transition temperature.

We define the energy density

$$\varepsilon=s\Theta-p+\mu_B n_B$$

and the entropy density

$$s=-\frac{\partial}{\partial\Theta}\left(\frac{\Omega}{V}\right)=\frac{\partial p}{\partial\Theta}.$$

The latent-heat density is

$$\Delta\varepsilon_d\equiv\varepsilon_1-\varepsilon_2=\Theta_d\Delta s_d\quad(\Theta=\Theta_d),$$

where $\Delta s_d\equiv s_1-s_2$ is the entropy-density jump at $\Theta=\Theta_d$.

For the considered case we have

$$s_1=(4A+C)\Theta^3,\quad s_2=\frac{2\pi^2}{15}\Theta^3,$$

with the notation

$$C\equiv\Theta\frac{\partial A}{\partial\Theta}=-\frac{33-2N_f}{24\pi^2}g^4\left[A_2+\frac{3}{2}A_3 g+\frac{1}{2}A_4(1+4\ln g)g^2\right],$$

where the equation

$$\frac{\partial g^2}{\partial\Theta}=-\frac{33-2N_f}{24\pi^2\Theta}g^4$$

is taken into account. The energy densities are

$$\varepsilon_1=(3A+C)\Theta^4+B,\quad \varepsilon_2=\frac{\pi^2}{10}\Theta^4.$$

Thus, for the latent heat one gets

$$\Delta\varepsilon_d=4B\left(1+\frac{C}{4}\gamma^4\right).$$

The nonperturbative term B is usually treated as the bag constant, with $B^{1/4}$ in the interval 150–300 MeV. For estimates, we can adopt the value $B^{1/4}=225$ MeV from the middle of this interval.

One often assumes that the quark–gluon plasma is an ideal gas of free quarks and gluons, that is, $g=0$. If this is so, then for $N_f=2$ we have $\gamma=0.72$. The deconfinement occurs at $\Theta_d=162$ MeV, being a first-order transition with latent heat $\Delta\varepsilon_d=4B\approx1$ GeV/fm^3. This deconfinement temperature Θ_d almost coincides with the characteristic energy $E_0=157$ MeV discussed in the Introduction. This picture would seem quite reasonable if it were not absolutely wrong. In reality, the effective coupling is $g(\Theta)\to\infty$ for temperatures Θ close to the scale parameter $\Lambda\approx200$ MeV. Therefore, the assumption that in the vicinity of the deconfinement point the quark–gluon plasma is an ideal gas of quarks and gluons is senseless. This would happen only at temperatures at which $g^2(\Theta)\ll1$, that is, when

$$\Theta\gg\Lambda\exp\left(\frac{24\pi^2}{33-2N_f}\right).$$

The latter inequality becomes valid only at very high temperatures $\Theta\gg10^6$ MeV.

Thus, nonperturbative effects around the deconfinement transition are very strong, and it is not correct to try to take them into account by the simple addition to the grand potential of a term B.

Some nonperturbative effects can be included by resorting to the effective-spectrum approximation,[31,32] when one postulates for the spectra of quarks and gluons the form $\varepsilon_i(k)=\sqrt{k^2+m_i^2}+U_i$, in which k is the modulus of the momentum, m_i is a mass, U_i is an effective mean field, and $i=q,g$ labels the quarks and gluons. This approximation yields results similar to the ideal-gas picture: The deconfinement is a first-order transition occurring at $\Theta\approx160$ MeV.

The reason why the effective-spectrum and ideal-gas approximations are close to each other can be understood as follows. The effective-spectrum approximation can be interpreted as a result of a renormalization of perturbative series. As an example, we can use self-similar renormalization,[33–36] differing from other resummation techniques by the possibility of checking its range of applicability at each step. We consider the coefficient A in the grand potential Ω_1 of the quark–gluon plasma as an effective limit of the sequence $\{f_k(g)\}$ with the initial approximation $f_0(g)=A_0+A_2g^2$, the first approximation $f_1(g)=f_0(g)+A_3g^3$, and so on. The simplest variant of self-similar renormalization[33–36] gives the renormalized coefficient

$$A^*=A_0+\frac{4A_2^3g^2}{(A_3g-2A_2)^2}.$$

This quantity, for $A_2<0$, is finite for all g, including $g\to\infty$. In the whole interval $g\in[0,\infty)$ the deconfinement temperature does not change much: for $g=0$ with $N_f=2$ it is $\Theta_d=162$ MeV, while for $g\to\infty$ it is $\Theta_d=176$ MeV. However, the renormalized value A^* is correct only when the self-similar renormalization is stable.[37–40] For this, the corresponding mapping multiplier $M_1(g)$ and the Lyapunov exponent $\Lambda_1(g)$ must satisfy the stability conditions $|M_1(g)|<1$ and $\Lambda_1(g)<0$. In the considered case,

$$M_1(g)=1+\Lambda_1(g),\quad \Lambda_1(g)=\frac{3A_3}{2A_2}g.$$

The Lyapunov exponent is always negative, since $A_2<0$ and $A_3>0$. The condition $|M_1(g)|<1$ holds only for $g<4|A_2|/3A_3$, that is, for $g\leqslant 1$.

Thus, the renormalization of the grand potential, starting from the perturbative expression, does not essentially change the results. And it is clear why: In reality, the ideal-gas picture, which forms the basis of the perturbative expansion, contains no information on bound states that should appear as the coupling constant g increases. The situation with the quark–gluon plasma is somewhat similar to that of the electron–ion plasma in which there can exist bound as well as free electron states.[41]

The value of the deconfinement temperature obtained in pure phase models can be quite reasonable, in the same way as for the simple estimate of the Introduction. However, it would be hard to believe that these models can correctly describe the character of the deconfinement transition and the behavior of thermodynamic functions.

4. LATTICE NUMERICAL SIMULATION

The idea of using a discrete space-time lattice to regularize quantum field theories opened the entire repertory of statistical physics for the analysis of nonperturbative properties of these theories. The application of Monte Carlo simulation techniques turned out to be a powerful approach making it possible to perform a quantitative study of nonperturbative aspects of quantum chromodynamics. The lattice reformulation of QCD has been described in several surveys (e.g., Refs. 4, 29, and 42); therefore below we only slightly touch upon the principal points of this approach. We shall mainly discuss the predictions of lattice QCD and its simplified variants for the deconfinement transition.

The first step towards the finite-temperature study of QCD consists of introducing the imaginary time $t=-i\tau$ and of rewriting the partition function as a path integral of the exponential of the Euclidean Lagrangian density over all fields in the problem. The second step defines the cubic four-dimensional lattice with the sites $x=\{\mathbf{x},\tau\}$ where $\mathbf{x}\in\mathbb{Z}_3$ is a real-space lattice vector and $\tau\in\mathbb{Z}_1$ is conventionally called the temporal variable. The lattice spacings in the spatial and temporal directions are denoted by a_σ and a_τ, respectively. If N_σ and N_τ are the numbers of sites in the corresponding directions, then the volume V and the temperature Θ of the system are given by $V\equiv(N_\sigma a_\sigma)^3$ and $\beta\equiv N_\tau a_\tau$, where $\beta\equiv\Theta^{-1}$.

A gauge-invariant theory on the lattice is usually formulated in terms of link variables U_x^μ and site variables $\psi(x)$ and $\bar{\psi}(x)$. The link variable U_x^μ is associated with a link leaving site x in a direction $\mu=1,2,3,4$ and is a matrix $U_x^\mu\in SU(N_c)$ in the space of color indices, N_c being the number of colors. The site variables $\psi(x)$ and $\bar{\psi}(x)$ are associated with each site x of the lattice and carry color, flavor, and spin indices. Also, $\psi(x)$ and $\bar{\psi}(x)$, representing fermion fields, are treated as Grassmann variables. The link and the site variables satisfy the periodicity conditions

$$U_{\mathbf{x},0}^\mu=U_{\mathbf{x},\beta}^\mu,\quad \psi(\mathbf{x},0)=-\psi(\mathbf{x},\beta).$$

Then, in terms of these variables, the partition function is written in the form of a path integral

$$Z=\int\prod_x\prod_\mu\prod_{x'}e^{-S}dU_x^\mu d\psi(x')d\bar{\psi}(x'),$$

in which the action

$$S=S(U_x^\mu,\psi(x')\bar{\psi}(x'))=S_G+S_F$$

consists of a gauge action S_G and a fermionic action S_F. The partition function and other thermodynamic functions are calculated by using the Monte Carlo procedure on a finite lattice of $N_\sigma^3\times N_\tau$ sites, the maximal number of sites in each direction being around $N_\sigma=24$ and $N_\tau=24$.

The deconfinement transition has been studied in lattice QCD or its pure gauge variants by many authors. Here we cite only some review-type papers.[43–52] Note that in addition to the confinement transition, another transition related to the spontaneous breaking of chiral symmetry can occur. The mechanisms leading to these transitions are seemingly unrelated, and thus it has been speculated that QCD may undergo two separate phase transitions. However, the Monte Carlo data for pure gauge models and for the variants with massless quarks suggest that these two transitions coincide. And if the finite masses of the quarks are taken into account, then the chiral symmetry, strictly speaking, occurs only in the limit $\Theta\to\infty$. In what follows we shall speak solely about the deconfinement transition. One of the main discoveries of the lattice simulation has been the fact that the deconfinement can be of quite different character for different systems.

SU(2) pure gauge model. The common convention is that the deconfinement for such quarkless models is a *second-order transition* occurring at $\Theta_d\approx 210$ MeV. The errors in calculating the pressure and energy density, related to the finiteness of the employed lattice, are around 5% above and 30% below Θ_d.

SU(3) pure gauge model. The deconfinement has been found to be a *first-order transition* at $\Theta_d\approx 225$ MeV with latent heat $\Delta\varepsilon_d\approx\frac{1}{4}\varepsilon_1(\Theta_d)$. The errors in calculating the pressure, energy density, and entropy are about 10% above and 30% below Θ_d.

SU(3) model with quarks. In the presence of dynamical fermions the situation is far more complicated, as it is difficult to perform high-statistics analysis of full QCD on large lattices that would allow a detailed finite-size study, as has now been done in the pure gauge sector. Monte Carlo simulations for full QCD with dynamical quarks have now been performed only for the case of zero baryon density. The transition has been found to be rather sensitive to the choice of quark masses and the number of flavors. It seems that for $N_f>4$ the transition is of first order for all quark masses. For $N_f\leqslant 4$ the situation is still to some extent uncertain. Nonetheless, there are strong indications that for physical quark masses and $N_f=3$ the transition is likely to be a continuous crossover, occurring at $\Theta_d\approx 150$ MeV. However, we again stress the uncertainties in the determination of the order of the transition in Monte Carlo simulations with quarks, even at zero baryon density.

What has been found in the lattice simulations with certainty[52,53] is that nonperturbative effects are quite strong around the deconfinement transition, persisting until about $2\Theta_d$. Also, it is seen that no statistical bootstrap or pure

phase model is able to describe the variety of different transition orders discovered in the lattice simulations, since these models always predict a sharp first-order transition.

5. DYNAMICAL CONFINEMENT SCENARIO

Correlation functions and related susceptibilities are among the key tools used for investigating phase transitions.[54] This also applies to QCD correlation functions.[55] The latter have been intensively studied in lattice numerical simulations.[56–60] The results of these studies revealed nontrivial effects in the high-temperature phase connected with strong quark–antiquark correlations, which was interpreted[56–60] as the existence of hadronic modes, even at high $\Theta > \Theta_d$. De Tar[56] proposed that the high-temperature phase might be dynamically confined, in the sense that the long-range fluctuations are color-singlet modes, and that the poles and cuts in the linear response functions of the hadronic phase go over smoothly into those of the high-temperature one. This scenario of dynamical confinement presupposes that there is actually no transition at all, and that there is only a smooth crossover between hadronic matter and quark–gluon plasma.

It is conjectured[56] that the characterization of the plasma as a weakly interacting gas of quarks and gluons is valid only for short distances and short time scales of the order $1/\Theta$, but that at scales larger than $1/g^2\Theta$, where g^2 is the running QCD coupling, the plasma exhibits confining features similar to that of the low-temperature hadronic phase. The confinement scale, for instance, at $\Theta \approx 200$ MeV, is expected to be of order 1 fm and 10^{-24} sec.

Hatsuda and Kunihiro[61–64] considered the density–density correlation functions of quarks for the Nambu–Jona-Lasinio model with a QCD-motivated effective Lagrangian. They found precursory collective excitations existing in the high-temperature phase and corresponding to correlated $q\bar{q}$ pairs. This means that meson modes exist above as well as below the transition temperature. In fact, all the poles and cuts of the correlation functions in the momentum–energy representation are the same at all temperatures. Thus, quarks, antiquarks, and gluons should also exist in the low-temperature as well as in the high-temperature phase. Such precursor effects are analogous to pretransitional fluctuations in superconductors[65] or in superfluid He^3 (Ref. 66).

The gradual change of the excitation spectrum from hadronic states to quarks and gluons, and the survival of hadronic modes above the transition temperature, have been confirmed for QCD in the instanton-liquid approach[67] and in the magnetic-current approximation.[68] In the latter case, quarks are assumed to interact at high temperature solely through magnetic current–current interactions, the electric ones being screened.

The following picture[68] may serve as an intuitive illustration of the dynamical confinement:[56–60] The current–current interactions persist above Θ_d and force any quark–antiquark pair (and maybe every three-quark state) to correlate into color singlets. As the quarks are moving in the heat bath, the strings connecting them for color neutrality are constantly breaking and reforming, which can be interpreted as hadrons going in and out of the heat bath.

If the transition between the hadron matter and the quark–gluon plasma is a gradual crossover, as follows from the dynamical confinement scenario, then why in many lattice simulations is this transition found to be of first order? The answer to this question was suggested by Kogut *et al.*,[69] explaining the first order of this transition merely as due to the finite size of the lattice. Calculating thermodynamic characteristics, such as energy densities, and correlation functions for several lattices with the sizes $8^3\times4$, $12^3\times4$, $12^3\times6$, and $16^3\times4$, it has been found[69] that the quark–gluon plasma transition becomes less abrupt as the lattice size increases and the evidence for a first-order transition becomes weaker. Lengthy runs for $N_\sigma = 16$ showed no evidence for metastability, so that Kogut *et al.*[69] concluded that their results suggest that there is no abrupt transition at all, but only a smooth crossover phenomenon.

To describe the coexistence of gluons and glueballs above Θ_d for a quarkless $SU(2)$ system, De Grand and De Tar[57,58] proposed to write the grand potential as the sum

$$\Omega = \Omega_1 + \Omega_2,$$

$$\Omega_1 = -\Theta V \frac{\zeta_1}{2\pi^2} \int_{k_0}^{\infty} k^2 \ln[1 + n_1(\mathbf{k})]dk,$$

$$\Omega_2 = -\Theta V \frac{\zeta_2}{2\pi^2} \int_{0}^{k_0} k^2 \ln[1 + n_2(\mathbf{k})]dk,$$

where Ω_1 corresponds to gluons and Ω_2 to glueballs; ζ_i is a degeneracy factor; the Bose distribution $n_i(\mathbf{k}) = [\exp\{\beta\varepsilon_i(\mathbf{k})\} - 1]^{-1}$ contains the spectrum $\varepsilon_i(\mathbf{k}) = \sqrt{k^2 + m_i^2}$ with the mass $m_1 = 0$ for gluons and the mass $m_2 \approx 1000$ MeV for glueballs. The cutoff momentum k_0 is postulated, to fit lattice data, to be $k_0 \to \infty$ below Θ_d and $k_0 = 2.86\Theta_d[\Theta_d/(\Theta - \Theta_d)]^{0.3}$ above Θ_d. This phenomenological model describes only the second-order transition in pure $SU(2)$ systems. The temperature dependence of the cutoff momentum k_0 is too arbitrary to permit a straightforward generalization to systems containing quarks as well as various hadrons.

The main value of the dynamical confinement scenario is the clear understanding that hadron and quark–gluon degrees of freedom generally coexist.

6. CLUSTERED QUARK MODEL

A model in which quarks could coexist with three-quark clusters, that is, nucleons, has been suggested by Clark *et al.*[70] for zero temperature and considered by Bi and Shi[71] at finite temperatures. Nucleons and quarks in this model are intermixed inside the same system. This kind of mixture should be distinguished from the Gibbs mixture, in which different phases are separated in space, having only a common interphase boundary (see Ref. 15). The quark–nucleon mixture is rather similar to a binary liquid mixture.[72] A two-component system can, in general, stratify in space if there are no chemical reactions between the components. The quark–nucleon mixture does not stratify because of the possibility of formation and decay of nucleon clusters, which is taken into account by the relation $\mu_N = 3\mu_q$ between the nucleon, μ_N, and quark, μ_q, chemical potentials. Since it is

assumed that inside a nucleon bag and outside it the QCD vacuum is different, the nonstratified mixture corresponds to a nonuniform, or inhomogeneous, vacuum. In a certain sense it is similar to the twinking vacuum discussed in connection with the instanton-liquid picture of the QCD vacuum.[29] A nucleon can be interpreted as a droplet of a denser phase inside the rarified plasma phase. Nucleons among quarks are like fog drops in the air. Another analogy is magnetic bubbles in magnets.[73]

Clark *et al.*[70] used the excluded-volume approximation, in which the particles move not in the whole volume V but only in the free volume $V_0=V-N_N v_N$, where N_N is the number of nucleons of the volume v_N, defined by the bag model. This renormalizes the volume ($V\to\xi V$) by the factor $\xi\equiv V_0/V=1-\rho_N v_N$, where $\rho_N\equiv N_N/V$ is the nucleon density. Then, e.g., the baryon density takes the form

$$n_B=\xi\int\left[\frac{1}{3}\,\zeta_q\left(1-\frac{2\alpha_s}{\pi}\right)n_q(\mathbf{k})+\zeta_N n_N(\mathbf{k})\right]\frac{d\mathbf{k}}{(2\pi)^3},$$

in which, in addition to the geometrical interaction taken into consideration by the factor ξ, the perturbative quark–quark interaction is simulated by the factor $1-2\alpha_s/\pi$. The Fermi distributions $n_i(\mathbf{k})$ contain the free spectra $\omega_i(\mathbf{k})=\sqrt{k^2+m_i^2}-\mu_i$. The energy density reads

$$\varepsilon=\varepsilon_q+\varepsilon_N+B,$$

$$\varepsilon_q=\xi\zeta_q\left(1-\frac{2\alpha_s}{\pi}\right)\int\varepsilon_q(\mathbf{k})n_q(\mathbf{k})\,\frac{d\mathbf{k}}{(2\pi)^3},$$

$$\varepsilon_N=\xi\zeta_N\int\varepsilon_N(\mathbf{k})n_N(\mathbf{k})\,\frac{d\mathbf{k}}{(2\pi)^3},$$

where the nonperturbative energy is given by a bag constant B.

Comparing the grand potentials for this model with $B^{1/4}=171$ MeV and with those of the pure quark and pure nucleon phases, it was found that the mixed clustered matter is more profitable at $n_B>8n_{0B}$ and $\Theta\leqslant 50$ MeV. Of course, one should not take too seriously the numerical predictions of this model, which is too oversimplified to be realistic. For instance, pions and gluons are not considered here, although they should play an important role in the deconfinement transition. Thus, pion fields make a nucleon bag unstable at quite moderate density and temperature[74,75] close to those discussed in the Introduction.

The most valuable idea in the clustered quark model is that of a nonuniform vacuum containing local fluctuations such that nucleons can be formed floating in the surrounding quark matter.

7. STRING-FLIP POTENTIAL MODEL

An extreme realization of the dynamical confinement scenario is given by the string-flip potential model[76–81] based on the quantum-mechanical Hamiltonian

$$H(\mathbf{r}_1,\ldots,\mathbf{r}_N)=\sum_{i=1}^{N}\left(-\frac{\nabla_i^2}{2m}\right)+V(\mathbf{r}_1,\ldots,\mathbf{r}_N)$$

of nonrelativistic quarks. In the interaction term

$$V(\mathbf{r}_1,\ldots,\mathbf{r}_N)=\min\sum_{\langle ij\rangle}\Phi(r_{ij})\quad(r_{ij}\equiv|\mathbf{r}_i-\mathbf{r}_j|)$$

the minimum is taken over all ways to group N quarks into hadrons, so that the summation actually goes only over $\langle i,j\rangle$ pertaining to the same hadron consisting of 2, 3, 6, 9, 12, or 15 quarks. Using the variational wave function

$$\Psi(\mathbf{r}_1,\ldots,\mathbf{r}_N)=\exp\{-\beta V(\mathbf{r}_1,\ldots,\mathbf{r}_N)\}D(\mathbf{r}_1,\ldots,\mathbf{r}_N),$$

in which β is a variational parameter and $D(...)$ is a free Fermi-gas Slater determinant, one minimizes the energy $E(\beta)=(\Psi,H\Psi)/(\Psi,\Psi)$ with respect to β. This gives $\beta=\beta(\rho)$ as a function of density.

Variational Monte Carlo calculations for this model have been accomplished with the harmonic, $\Phi(r)=\frac{1}{2}m\omega^2r^2$, and linear, $\Phi(r)=\sigma r$, confining potentials. The wave function has been symmetrized with respect to all the quark coordinates, including those pertaining to different hadrons. This takes into consideration the exchange quark energy, which is found[82] to be about 100 MeV.

The results show that the quarks always coalesce into the lowest-energy set of flux tubes, which is characteristic of an adiabatic approximation to the strong-coupling limit of QCD. At low densities $\rho<\rho_0$ the quarks cluster into isolated hadrons. As the density increases, the value of $\beta(\rho)$ decreases, first slowly, but at $\rho\approx 1.5\rho_0$ exponentially. For $\rho\geqslant 2\rho_0$ the wave functions of separate hadrons strongly overlap, which may be interpreted as a transition to quark matter, although formally all the quarks are still confined. Complete deconfinement occurs at asymptotically high densities, when $\beta(\rho)\to 0$, and the wave function becomes that of a free Fermi gas of quarks.

The quark–quark pair correlation function was calculated[76,79] using Monte Carlo techniques, and the longitudinal response function was calculated using molecular-dynamics simulations.[83] At low densities these functions have the properties typical of a set of isolated hadrons. For instance, the pair correlation function has a sharp peak, displaying strong correlations between the quarks. The form of this function is similar to that of liquids.[84,85] As the density increases, the peak in the pair correlation function relaxes smoothly to that of a Fermi gas of quarks, disappearing completely as $\rho\to\infty$.

Thus, the string-flip model demonstrates a smooth transition from hadron matter at low densities to a free Fermi gas of quarks at high densities. Quarks at all densities are to some extent confined, becoming an absolutely free gas only in the limit $\rho\to\infty$.

The main difficulty in dealing with this model is the need to minimize the Hamiltonian interaction term over all strings connecting quarks, which involves complicated Monte Carlo calculations. This procedure is necessary for eliminating color van der Waals forces between color-singlet hadrons. These forces are present in confining two-body potentials and, if not eliminated, produce large spurious energies in nuclear matter.

However, in a consistent static approach this kind of divergence can be automatically canceled if one takes into account the corresponding correlation functions, called

smoothing or screening functions, which smooth the interaction potentials in the regions of their divergence.[86–88] It is possible, starting with divergent interaction potentials, to construct a regular iterative theory[35,89] for Green functions, each step of which involves only smoothed potentials containing no divergences. In the lower orders of this correlated iteration theory[35] the situation is such that it could be obtained by replacing from the beginning the bare interaction potential by a smoothed one, that is, by defining an effective Hamiltonian with a pseudopotential instead of the initial potential.[86] Such a replacement is an approximation neglecting some double and all triple correlations.[35]

The Hamiltonian of the string-flip model including the minimization over strings is an effective Hamiltonian, in which this minimization plays the role of smoothing. In lieu of this complicated minimization requiring Monte Carlo techniques, it is equivalent to replacing the confining potential by a smoothed one.

Röpke *et al.*[90–93] have developed a many-body approach to quark–nuclear matter, generalizing and simplifying the string-flip model. This approach starts with an effective Hamiltonian

$$H_{\rm eff}(\mathbf{r}_1,\ldots,\mathbf{r}_N)=\sum_{i=1}^{N}\left(m_i-\frac{\nabla_i^2}{2m_i}\right)+\frac{1}{2}\sum_{i,j}^{N}V_{\rm eff}(\mathbf{r}_{ij}),$$

in which m_i stands for the quark masses, and the effective interaction $V_{\rm eff}(\mathbf{r})\equiv s(r)\Phi(r)$ is screened by a function $s(r)$ defining the probability that two quarks at distance r are next neighbors. The screening function is found from some additional equations. In the case of independent particles with density ρ, one has $s(r)=\exp(-(4\pi/3)\rho r^3)$. Inside a hadron, when $r\ll a$, where $a\equiv\rho^{-1/3}$ is an average interquark distance in the system, we have $s(r)\simeq 1$, so that quarks interact through a bare confining potential. For the quarks pertaining to different hadrons, i.e., when $r\gg a$, we get $s(r)\simeq 0$, which is called the saturation property.[91]

The many-body approach to clustering quark matter[90–93] makes it possible to give a unique description of the clustered hadrons as well as the free-quark phase in the same way as has been done for nuclear matter whose nucleons could form the deuteron, triton, and α-particle bound states.[94,95] The total density of clustering matter is a sum $\rho=\Sigma_i z_i\rho_i$, in which z_i is a compositeness factor and ρ is the density of the i component of clusters composed of z_i particles.

In the many-body approach the quark system may contain both quasifree quarks (scattering states) and various clusters (bound states). At zero temperature, nucleons start dissolving at $n_B\approx 4.3n_{0B}$. At zero baryon density the transition of hadron matter to the free-quark phase starts at $\Theta_d\approx 200$ MeV, where some of the meson states are already dissolved. But other bound quark states do still exist at this temperature. The dissolution of the bound states occurs gradually with temperature. Some mesons survive up to $\Theta\approx 2\Theta_d$. The gradual dissociation of bound states above Θ_d is in agreement with the dynamical deconfinement scenario.

Although the many-body approach provides the principal possibility of treating bound states together with quasifree ones, it has the following technical obstacles. Each bound state is described by a Bethe–Goldstone-type equation for a two- or three-particle Green function, depending on the compositeness of this bound state. This type of equation, as is well known, is very difficult to deal with. When there are many bound states interacting with each other as well as with unbound particles, one has to deal with a system of many interrelated Bethe–Goldstone equations, in addition to several equations for one-particle Green functions. In such a case the problem becomes practically as difficult as chromodynamics itself.

8. CONCEPT OF CLUSTER COEXISTENCE

As follows from the previous sections, there is a need for a statistical model that could provide a realistic description of clustering matter, which is at the same time treatable. One almost evident simplification would be, instead of suffering with a system of Bethe–Goldstone equations, to consider bound clusters as separate objects. This can be understood as a kind of renormalization by integrating out the internal degrees of freedom corresponding to the motion of particles inside each of the clusters, so that only the center-of-mass degrees of freedom are left.

We enumerate all possible cluster states, including those of unbound, or free, particles, by the index i. Let $\psi_i(\mathbf{r})=[\psi_i^\alpha(\mathbf{r})]$ be the field operator of an i cluster, this operator being a column in the space of quantum degrees of freedom indexed by α. The quantum degrees of freedom include spin, isospin, color, and flavor indices. The field operators satisfy the commutation relations

$$[\psi_i^\alpha(\mathbf{r}),\psi_j^\gamma(\mathbf{r}')]_\mp=0,\quad [\psi_i^\alpha(\mathbf{r}),\psi_j^{\dagger\gamma}(\mathbf{r}')]_\mp=\delta_{ij}\delta_{\alpha\gamma}\delta(\mathbf{r}-\mathbf{r}'),$$

where the upper sign stands for Bose and the lower sign for Fermi statistics.

We take an effective Hamiltonian in the form

$$H=\hat{E}-\sum_i \mu_i\hat{N}_i, \tag{1}$$

in which the energy operator

$$\hat{E}=\sum_i \hat{E}_i+\sum_{i,j}\hat{E}_{ij} \tag{2}$$

consists of the single-cluster energies

$$\hat{E}_i=\int \psi_i^\dagger(\mathbf{r})K_i(\nabla)\psi_i(\mathbf{r})d\mathbf{r}, \tag{3}$$

where $K_i(\nabla)$ is the kinetic-energy operator, and of the interaction energies

$$\hat{E}_{ij}=\frac{1}{2}\int \psi_i^\dagger(\mathbf{r})\psi_j^\dagger(\mathbf{r}')\Phi_{ij}(\mathbf{r}-\mathbf{r}')\psi_j(\mathbf{r}')\psi_i(\mathbf{r})d\mathbf{r}d\mathbf{r}', \tag{4}$$

in which the interaction potentials $\Phi_{ij}(\mathbf{r})$ have the symmetry property

$$\Phi_{ij}(\mathbf{r})=\Phi_{ij}(-\mathbf{r})=\Phi_{ji}(\mathbf{r}). \tag{5}$$

In the second term of (1), μ_i is the chemical potential of the i clusters and

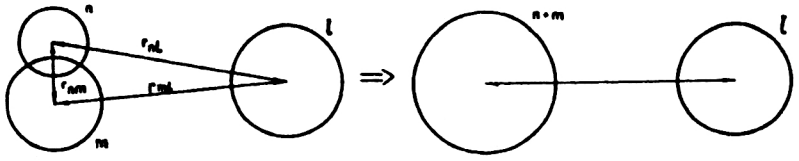

FIG. 1. Illustration of cluster fusion.

$$\hat{N}_i = \int \psi_i^\dagger(\mathbf{r})\psi_i(\mathbf{r})d\mathbf{r} \tag{6}$$

is the number-of-clusters operator.

The grand potential

$$\Omega = -\Theta \ln \mathrm{Tr}\, e^{-\beta H} \tag{7}$$

defines the pressure

$$p \equiv -\frac{\Omega}{V} = \frac{\Theta}{V} \ln \mathrm{Tr}\, e^{-\beta H}. \tag{8}$$

The energy density is given by

$$\varepsilon \equiv \frac{1}{V}\langle \hat{E} \rangle, \tag{9}$$

where $\langle ... \rangle$ denotes statistical averaging.

For each kind of cluster we can define their density

$$\rho_i(\mathbf{r}) = \langle \psi_i^\dagger(\mathbf{r})\psi_i(\mathbf{r}) \rangle, \tag{10}$$

the number of clusters

$$N_i \equiv \langle \hat{N}_i \rangle = \int \rho_i(\mathbf{r})d\mathbf{r}, \tag{11}$$

and the average density

$$\rho_i \equiv \frac{N_i}{V} = \frac{1}{V}\int \rho_i(\mathbf{r})d\mathbf{r}. \tag{12}$$

The number of constituents of an i cluster is called the compositeness factor z_i. The total number of elementary particles is

$$N = \sum_i z_i N_i, \tag{13}$$

so that the average density of the system can be written as

$$\rho \equiv \frac{N}{V} = \sum_i z_i \rho_i. \tag{14}$$

The chemical potentials μ_i can be determined from the conservation laws accepted for the given system. For example, if the numbers N_i for each sort of cluster are fixed, then (12) gives $\mu_i(\Theta, \rho_i)$. If the total number of constituents (13) is fixed, then from the equilibrium condition $\delta\Omega = 0$ we have

$$\frac{\mu_i}{z_i} = \frac{\mu_j}{z_j}, \tag{15}$$

which, together with (14), determines $\mu_i(\Theta, \rho)$. When neither N_i nor N is fixed, $\mu_i = 0$.

An important quantity is the *cluster probability*

$$w_i \equiv z_i \frac{\rho_i}{\rho} = z_i \frac{N_i}{N} \tag{16}$$

obeying the conditions

$$0 \leq w_i \leq 1, \quad \sum_i w_i = 1, \tag{17}$$

following from (14). With (12), we may rewrite (16) as

$$w_i = \frac{z_i}{N}\int \rho_i(\mathbf{r})d\mathbf{r}. \tag{18}$$

If the system of particles can form a number of bound states, how can we determine the numerous interactions between clusters? The number of such interactions can be drastically reduced for those clusters whose interaction potentials $\Phi_{ij}(\mathbf{r})$ have the same type of behavior at large distance, for example, diminishing as r increases. Consider such clusters with a similar behavior of $\Phi_{ij}(\mathbf{r})$. Let two clusters, m and n, coalesce into one, i, so that the compositeness numbers involved in the reaction $m + n \to i$ satisfy the obvious relation $z_m + z_n = z_i$. Suppose that there is another cluster spectator, j, as shown in Fig. 1. Assume that the coalescence of the active clusters does not influence the cluster spectator, in the sense that its interaction with the initial two clusters is the same as the interaction with the one formed after the coalescence:

$$\Phi_{mj}(\mathbf{r}) + \Phi_{nj}(\mathbf{r}) = \Phi_{ij}(\mathbf{r}). \tag{19}$$

From this assumption, using the conservation law $z_m + z_n = z_i$, we find the relation

$$\frac{\Phi_{ij}(\mathbf{r})}{z_i z_j} = \frac{\Phi_{mn}(\mathbf{r})}{z_m z_n}, \tag{20}$$

permitting us to express the interaction potentials of different clusters in terms of one calibration potential.

9. SCREENING OF INTERACTION POTENTIALS

The interaction potential $\Phi_{ij}(\mathbf{r})$ may be divergent for some regions of $\mathbf{r}$. However, it would not be correct to replace this potential by a smoothed, or screened, one just in the Hamiltonian (1). Such a screening appears in the process of decoupling of binary propagators with allowance for interparticle correlations, as is done in the correlated iteration theory.[35] If one wishes to write an effective Hamiltonian corresponding to a given correlated approximation, it is not sufficient to merely rearrange the operator terms of the Hamiltonian; a nonoperator correcting term must be added.

Let us illustrate this for the correlated mean-field approximation,[35] in which the Hamiltonian (1) can be represented in the form

$$H=\sum_i H_i+CV,$$

$$H_i=\int \psi_i^\dagger(\mathbf{r})[K(\nabla)+U_i(\mathbf{r})-\mu_i]\psi_i(\mathbf{r})d\mathbf{r}, \tag{21}$$

in which the correlated mean field

$$U_i(\mathbf{r})=\sum_j \int \bar{\Phi}_{ij}(\mathbf{r}-\mathbf{r}')\rho_j(\mathbf{r}')d\mathbf{r}' \tag{22}$$

contains the screened potential

$$\bar{\Phi}_{ij}(\mathbf{r})=s_{ij}(\mathbf{r})\Phi_{ij}(\mathbf{r}) \tag{23}$$

smoothed by a smoothing function having the symmetry property

$$s_{ij}(\mathbf{r})=s_{ji}(\mathbf{r})=s_{ij}(-\mathbf{r}). \tag{24}$$

The nonoperator correcting term in (21) is CV, and this cannot be put equal to zero, as will be shown below.

Since the exact Hamiltonian (1) does not depend on the cluster densities, by varying the grand potential (7) with respect to $\rho_i(\mathbf{r})$ we have

$$\frac{\delta\Omega}{\delta\rho_i(\mathbf{r})}=\left\langle\frac{\delta H}{\delta\rho_i(\mathbf{r})}\right\rangle=0. \tag{25}$$

In order that the exact Hamiltonian (1) be correctly represented by the approximate Hamiltonian (21), we require that the latter satisfy (25), which yields

$$\frac{\delta C}{\delta\rho_i(\mathbf{r})}+\frac{1}{V}\sum_j\left\langle\frac{\delta H_j}{\delta\rho_i(\mathbf{r})}\right\rangle=0. \tag{26}$$

The substitution

$$\left\langle\frac{\delta H_i}{\delta\rho_i(\mathbf{r})}\right\rangle=\int\frac{\delta U_j(\mathbf{r}')}{\delta\rho_i(\mathbf{r})}\rho_i(\mathbf{r}')d\mathbf{r}',$$

transforms (26) into

$$\frac{\delta C}{\delta\rho_i(\mathbf{r})}+\frac{1}{V}\sum_j\int\frac{\delta U_j(\mathbf{r}')}{\delta\rho_i(\mathbf{r})}\rho_j(\mathbf{r}')d\mathbf{r}'=0. \tag{27}$$

If the smoothing function $s_{ij}(\mathbf{r})$ does not depend on $\rho_i(\mathbf{r})$, then (22) gives

$$\frac{\delta U_i(\mathbf{r})}{\delta\rho_j(\mathbf{r}')}=\bar{\Phi}_{ij}(\mathbf{r}-\mathbf{r}').$$

Equation (27) becomes

$$\frac{\delta C}{\delta\rho_i(\mathbf{r})}+\frac{1}{V}\sum_j\int\bar{\Phi}_{ij}(\mathbf{r}-\mathbf{r}')\rho_j(\mathbf{r}')d\mathbf{r}'=0.$$

The solution of the latter variational equation, apart from a constant that can be omitted, is

$$C=-\frac{1}{2V}\sum_{i,j}\int\bar{\Phi}_{ij}(\mathbf{r}-\mathbf{r}')\rho_i(\mathbf{r})\rho_j(\mathbf{r}')d\mathbf{r}d\mathbf{r}'.$$

Note that the Hamiltonian (21) with the given correcting term could be derived from (1) with the substitution

$$\psi_i^\dagger(\mathbf{r})\psi_j^\dagger(\mathbf{r}')\psi_j(\mathbf{r}')\psi_i(\mathbf{r})\to s_{ij}(\mathbf{r}-\mathbf{r}')\{\psi_i^\dagger(\mathbf{r})\psi_i(\mathbf{r})\rho_j(\mathbf{r}')$$
$$+\rho_i(\mathbf{r})\psi_j^\dagger(\mathbf{r}')\psi_j(\mathbf{r}')$$
$$-\rho_i(\mathbf{r})\rho_j(\mathbf{r}')\},$$

corresponding to the correlated Hartree approximation.[35]

In general, the smoothing function $s_{ij}(\mathbf{r})$ depends on $\rho_i(\mathbf{r})$. Therefore, the correcting term must be found from Eq. (26) or (27). In any case, the correcting term depends on thermodynamic variables through the densities $\rho_i(\mathbf{r})$. Thus, neglect of this term would distort the correct statistical description, and the behavior of the thermodynamic functions could be completely spoiled.

Let us pass to a uniform system with $\rho_i(\mathbf{r})=\rho_i$. In principle, a multicomponent system can display a variety of nonuniform states related to the solidification of one or several components. For example, an ensemble of fully ionized nuclei can form a crystalline lattice immersed in a uniform electron background, which models the high-density matter of white dwarfs.[96] It may be that some heavy cluster components crystallize, while others are liquid-like, as in superionic conductors.[97] It also may be that heavy clusters form an amorphous solid, while light ones move in a conduction band, as in glassy metals.[98] In the cores of neutron stars a Gibbs mixture can exist, when in some volumes of space a lattice structure appears, while others are filled by liquid-like nuclear matter.[99] We leave aside all these possibilities, considering in what follows only uniform systems.

In the uniform case, the mean field (22) becomes

$$U_i(\mathbf{r})=\sum_j\Phi_{ij}\rho_i\equiv U_i \tag{28}$$

with the interaction integral

$$\Phi_{ij}\equiv\int\bar{\Phi}_{ij}(\mathbf{r})d\mathbf{r}. \tag{29}$$

Instead of (25), we have

$$\left\langle\frac{\delta H}{\delta\rho_i}\right\rangle=0. \tag{30}$$

The correcting equation (27), defining the correcting term, changes to

$$\frac{\delta C}{\delta\rho_i}+\sum_j\frac{\delta U_j}{\delta\rho_i}\rho_j=0. \tag{31}$$

The field operators for a uniform system can be expanded in plane waves:

$$\psi_i(\mathbf{r})=\frac{1}{\sqrt{V}}\sum_k a_i(\mathbf{k})e^{i\mathbf{k}\cdot\mathbf{r}};\quad a_i(\mathbf{k})=[a_i^\alpha(\mathbf{k})].$$

Then the i-cluster Hamiltonian in (21) transforms to

$$H_i=\sum_k\omega_i(\mathbf{k})a_i^\dagger(\mathbf{k})a_i(\mathbf{k}), \tag{32}$$

with the effective spectrum

$$\omega_i(\mathbf{k})\equiv\varepsilon_i(\mathbf{k})-\mu_i,\quad \varepsilon_i(\mathbf{k})\equiv K_i(\mathbf{k})+U_i. \tag{33}$$

The number of clusters (11) reads

$$N_i=\sum_k \langle a_i^\dagger(\mathbf{k})a_i(\mathbf{k})\rangle=\zeta_i\sum_k n_i(\mathbf{k}), \tag{34}$$

where ζ_i is the degeneracy factor, i.e., the number of quantum states, and

$$n_i(\mathbf{k})=\{\exp[\beta\omega_i(\mathbf{k})]\mp 1\}^{-1} \tag{35}$$

is the Bose (upper sign) or Fermi (lower sign) momentum distribution. The cluster density (12) is

$$\rho_i=\zeta_i\int n_i(\mathbf{k})\,\frac{d\mathbf{k}}{(2\pi)^3}. \tag{36}$$

For the grand potential (7) one gets

$$\Omega=\sum_i \Omega_i+CV,$$

$$\Omega_i=\mp\Theta V\zeta_i\int \ln[1\pm n_i(\mathbf{k})]\,\frac{d\mathbf{k}}{(2\pi)^3}. \tag{37}$$

The pressure (8) becomes

$$p=\sum_i p_i-C,$$

$$p_i=\pm\Theta\zeta_i\int \ln[1\pm n_i(\mathbf{k})]\,\frac{d\mathbf{k}}{(2\pi)^3}. \tag{38}$$

The energy density (9) is

$$\varepsilon=\sum_i \varepsilon_i+C,$$

$$\varepsilon_i=\zeta\int \varepsilon_i(\mathbf{k})n_i(\mathbf{k})\,\frac{d\mathbf{k}}{(2\pi)^3}. \tag{39}$$

The cluster probability (18) becomes

$$w_i=\frac{z_i}{\rho}\,\zeta_i\int n_i(\mathbf{k})\,\frac{d\mathbf{k}}{(2\pi)^3}. \tag{40}$$

An additional simplification appears for the case of isotropic systems, which is usually assumed, when $\varepsilon_i(\mathbf{k})=\varepsilon_i(k)$, where $k\equiv|\mathbf{k}|$. Then $\omega_i(\mathbf{k})=\omega_i(k)$ and $n_i(\mathbf{k})=n_i(k)$. If the spectrum $\omega_i(k)$ is such that the asymptotic properties

$$k^3\ln\omega_i(k)\to 0 \quad (k\to 0),$$

$$\omega_i(k)\to\infty \quad (k\to\infty)$$

hold, then the cluster pressure and the cluster energy density reduce to

$$p_i=\frac{\zeta_i}{6\pi^2}\int_0^\infty k^3\varepsilon_i'(k)n_i(k)dk,$$

$$\varepsilon_i=\frac{\zeta_i}{2\pi^2}\int_0^\infty k^2\varepsilon_i(k)n_i(k)dk,$$

where $\varepsilon_i'(k)\equiv d\varepsilon_i(k)/dk$.

These are the basic formulas which we shall use in what follows.

10. COEXISTING MULTIQUARK CLUSTERS

The concept of cluster coexistence was first applied to nuclear matter consisting of different multiquark clusters. The interest in this problem was motivated by the Baldin cumulative effect[1] and the related discussion of the possible existence of multiquark clusters in nuclei.[100,101]

Since at high density or temperature relativistic effects play an important role, the kinetic term of the cluster spectra is taken in the relativistic form $K_i(\mathbf{k})=\sqrt{k^2+m_i^2}$, where m_i is the cluster mass. A system of 3-, 6-, 9-, and 12-quark clusters has been considered in the excluded-volume approximation.[102–106] The 3 and 9 quarks are fermions, and the 6 and 12 quarks are bosons. The bosons with the lowest mass, that is, the 6 quarks, can drop down in the Bose–Einstein condensate, when $\omega_6(0)=0$, which fixes μ_6. The chemical potentials always satisfy (15).

In the excluded-volume approximation the interaction between clusters is considered geometrically by putting Φ_{ij} equal to zero, but replacing the total volume V by the free volume V_0,

$$V\to V_0\equiv V-\sum_i N_i v_i, \tag{41}$$

where v_i are the cluster volumes. This reduces the volume

$$V\to\xi V;\quad \xi\equiv\frac{V_0}{V}=1-\sum_i \rho_i v_i, \tag{42}$$

by a factor $\xi\in[0,1]$. Equivalently, this can be interpreted as a reduction of the degeneracy factor

$$\zeta_i\to\tilde{\zeta}_i\equiv\xi\zeta_i. \tag{43}$$

The reduction factor in (42) and (43) can also be written as

$$\xi=\left(1+\sum_i \rho_i^{(0)}v_i\right)^{-1};\quad \rho_i^{(0)}\equiv\zeta_i\int n_i(k)\,\frac{d\mathbf{k}}{(2\pi)^3}.$$

Thus, for the density of clusters, the pressure, and the energy density one has

$$\rho_i=\tilde{\zeta}_i\int n_i(k)\,\frac{d\mathbf{k}}{(2\pi)^3},$$

$$p=\pm\Theta\sum_i \tilde{\zeta}_i\int \ln[1\pm n_i(k)]\,\frac{d\mathbf{k}}{(2\pi)^3},$$

$$\varepsilon=\sum_i \tilde{\zeta}_i\int \varepsilon_i(k)n_i(k)\,\frac{d\mathbf{k}}{(2\pi)^3}. \tag{44}$$

The volumes of the clusters are assumed to be related by the equation

$$\frac{v_i}{m_i}=\frac{v_j}{m_j}. \tag{45}$$

This permits us to express all the cluster volumes $v_i=m_iv_3/m_3$ in terms of the 3-quark volume $v_3=4\pi r_3^3/3$ with the radius $r_3=0.4$ fm of the nucleon core.

The employed multiquark parameters are given in Table I. The 3 quark is a nucleon. The 6-quark mass $m_6=1944$ MeV corresponds to an average value over the masses of several light narrow dibaryons that are claimed to be ob-

TABLE I. Multiquark parameters.

Mass m_i (MeV)	Compositeness number z_i	Degeneracy factor ζ_i
939	3	4
1944	6	9
2163	6	3
3521	9	4
4932	12	1

served in experiments.[107] The mass $m_6=2163$ MeV is taken from the bag-model calculation of Jaffe,[108] and the 9- and 12-quark parameters are taken from the bag model of Matveev and Sorba.[109]

The 6-quark probability depends on the value of the mass m_6, as is illustrated in Fig. 2. The results for other cluster probabilities are displayed in Figs. 3 and 4, where $m_6=2163$ MeV. The probabilities of heavy clusters are always very small: $w_9<0.1$, $w_{12}<0.01$.

As we are limited here by the length of this review, we shall not discuss in detail the results of our calculations, which can be found in the cited papers. We think that our figures speak for themselves: it is better to see once than to listen a hundred times.

The coexistence of nucleons with 6-quark clusters has also been considered in the mean-field approximation[110] with the effective interaction potential

$$\Phi_{ij}(\mathbf{r})=2\pi\frac{a_{ij}}{m_{ij}}\delta(\mathbf{r})-\frac{\alpha_\pi}{r}\exp(-m_\pi r).$$

The first term here is the Fermi pseudopotential for the core interaction with the scattering length $a_{ij}\equiv\frac{1}{2}(a_i+a_j)$, where $a_i\equiv a_{ii}$, and with the reduced mass $m_{ij}\equiv m_i m_j/(m_i+m_j)$. The second term is due to one-pion exchange, where $\alpha_\pi=0.08$ is the pion coupling parameter and $m_\pi=140$ MeV is the pion mass. Again, to reduce the number of model parameters, the relation $a_i^3/m_i=a_j^3/m_j$, similar to (45), is adopted. Then all the scattering lengths $a_i=a_3(m_i/m_3)^{1/3}$ are expressed in terms of the nucleon scattering length $a_3=1.6$ fm. The $6q$ probability is shown in Fig. 5.

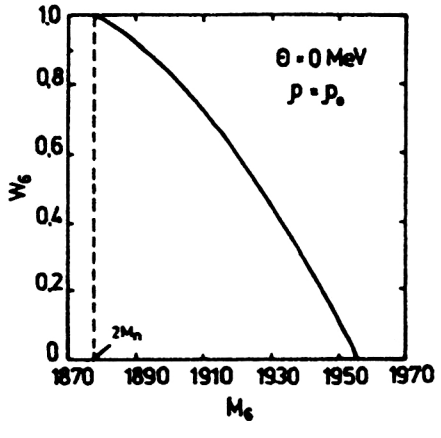

FIG. 2. $6q$ probability vs the mass of a $6q$ cluster at $\Theta=0$ and $\rho=\rho_0$.

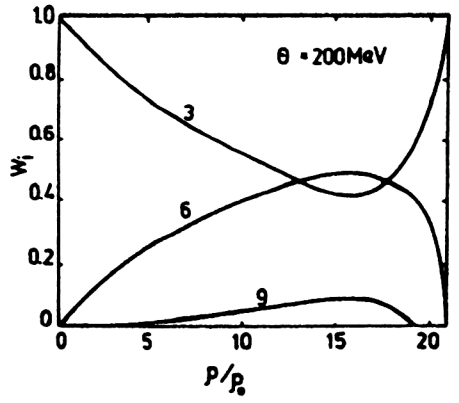

FIG. 3. Cluster probabilities as functions of the relative density at $\Theta=200$ MeV.

Note that the mean-field approximation is valid if $|U_i|\ll m_i$, which is true for densities up to about $10\rho_0$.

The models of this section serve as a qualitative illustration of cluster coexistence. They can make sense only at temperatures and densities much lower than those characteristic of deconfinement, as unbound quarks are not included here.

11. BARYON-RICH MATTER

We take into consideration unbound (quasifree) quarks that can, in principle, coexist with multiquark clusters. Whether and when quasifree quarks really coexist should be determined in a self-consistent way from the conditions of thermodynamic advantageousness and stability. To compare the results with those of the previous section, we consider again the case of baryon-rich matter, when $\rho=3n_B$, that is, when the generation of particles from the vacuum can be neglected.

We denote the chemical potential of a quark by $\mu\equiv\mu_q$. Then the relation (15) yields $\mu_i=z_i\mu$.

The strengths of the characteristic interactions between baryons and between quarks are of the order of or higher than the expected deconfinement temperature, so that these

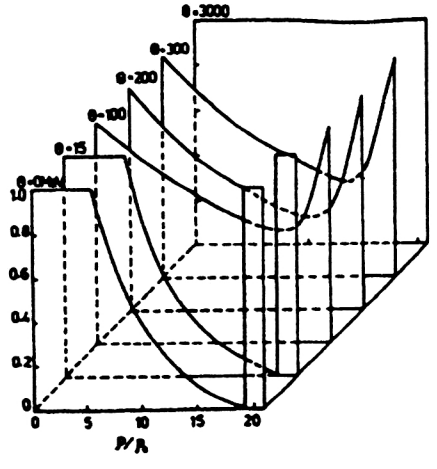

FIG. 4. Nucleon probability as a function of the relative density at different temperatures.

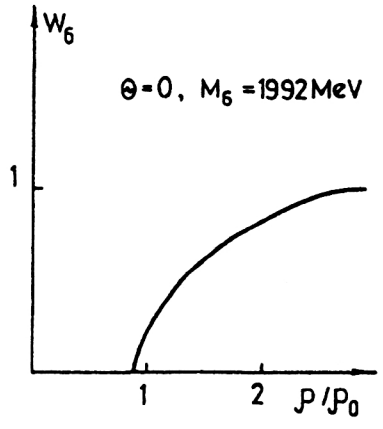

FIG. 5. $6q$ probability vs relative density at $\Theta=0$.

interactions must be taken into account. The mean field acting on the quarks can be written in a bag-model form[32] as $U_q=BV/N=B/\rho$. This gives for the quarks the spectrum

$$\varepsilon_q(k)=\sqrt{k^2+m_q^2}+\frac{B}{\rho}. \tag{46}$$

The mean-field term in (46) contains the total quark density ρ, which means that each quasifree quark interacts in the same way with the other unbound quarks as well as with the quarks entering into bound clusters. The interaction potentials between different baryons can be expressed on the basis of the relation (20) in terms of the nucleon–nucleon interaction potential $\Phi_{33}(\mathbf{r})$:

$$\Phi_{ij}(\mathbf{r})=\frac{z_i z_j}{9}\,\Phi_{33}(\mathbf{r}). \tag{47}$$

There are several such effective potentials obtained from nucleon–nucleon scattering experiments[111] or from analyses of the deuteron properties.[112] We opt for the Bonn potential.[113] The common consensus is that the thermodynamics of nuclear matter does not depend on the mutual orientation of the spins of the interacting nucleons. Averaging over the spin directions nullifies the spin terms of the interaction potential. The so-called cut-off terms of the Bonn potential can be neglected, since they start playing an essential role only for very short distances $\leqslant 0.1$ fm, which would correspond to baryon density $n_B \geqslant 10^3 n_{0B}$. We assume that the interaction between any pair of nucleons is the same, so that in the isospin term of the Bonn potential we put the total isospin $I_1+I_2=1$ describing the interaction between protons or neutrons. The radial part of the Bonn potential[113] then reads

$$\Phi_{33}(\mathbf{r})=\sum_{i=1}^{4}\frac{\alpha_i}{r}\exp(-\gamma_i r) \tag{48}$$

with the parameters

$$\alpha_1=16.7,\quad \alpha_2=2.7,\quad \alpha_3=-7.8,\quad \alpha_4=-2.7,$$

$$\gamma_1=738\ \text{MeV},\quad \gamma_2=769\ \text{MeV},$$

$$\gamma_3=550\ \text{MeV},\quad \gamma_4=983\ \text{MeV}.$$

The interaction potential (48) is integrable; thus, it does not necessarily require the smoothing procedure.[35,88,114] For the interaction-energy density (29) we have

$$\Phi_{33}=\int \Phi_{33}(\mathbf{r})d\mathbf{r}, \tag{49}$$

which yields $\Phi_{33}=4.1\times10^{-5}\ \text{MeV}^{-2}=315\ \text{MeV}\cdot\text{fm}^3$. Note that $\Phi_{33}\rho_0=164$ MeV, and hence $\Phi_{33}\rho_0\approx E_0=\rho_0^{1/3}$, so that $\Phi_{33}\approx\rho_0^{-2/3}$.

For the spectra of baryons we take

$$\varepsilon_i(k)=\sqrt{k^2+m_i^2}+\frac{z_i}{9}(\rho-\rho_q)\Phi_{33}, \tag{50}$$

where ρ_q is the quark density and i labels the multiquark clusters: $3q$, $6q$, $9q$, $12q$, and so on. The masses of bound clusters up to $z_i=12$ are taken from Table I, with the six-quark mass $m_6=1944$ MeV. For $z_i\geqslant 15$ we use the formula $m_i\approx(z_i/3)m_3$ for the masses of heavy multiquark clusters.[22]

For the quarks we adopt the mass $m_q=7$ MeV and the degeneracy factor $\zeta_q=12$ corresponding to spin 1/2, $N_c=3$, and $N_f=2$. The bag constant is $B^{1/4}=235$ MeV.

The results of numerical calculations[115–119] are presented in Figs. 6–13. At $\Theta=0$ and $\rho=\rho_0$, the $6q$ probability is $w_6=0.18$, which agrees with the estimates of the $6q$ admixture in nuclei.[120] The heavy-multiquark probabilities are always small: $w_9<10^{-3}$, $w_{12}<10^{-5}$, and $w_{15}<10^{-7}$. At zero temperature, only Bose-condensed $6q$ clusters exist, the probabilities of heavier ones being strictly zero. Unbound quarks at $\Theta=0$ are absent below the density $\rho_q^{\text{nuc}}\approx 2\rho_0$, when they start appearing. This is why the characteristic density

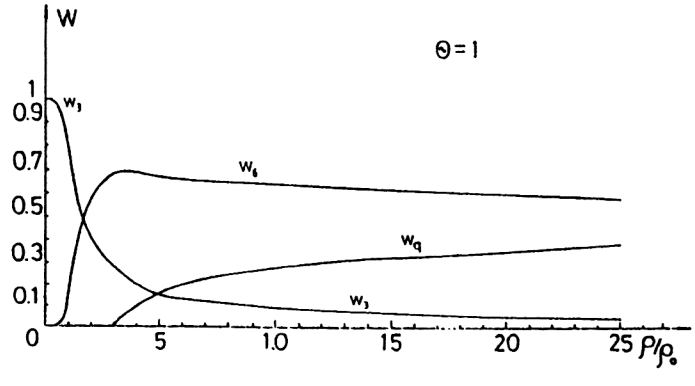

FIG. 6. Nucleon, $6q$-cluster, and unbound-quark probabilities as functions of the relative density at $\Theta=0$.

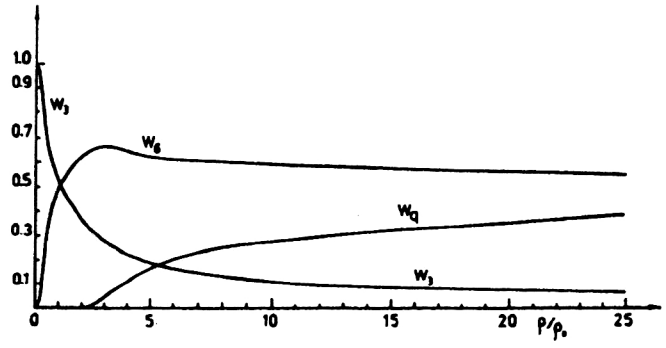

FIG. 7. Probabilities of unbound quarks and of bound clusters vs relative density at $\Theta=30$ MeV.

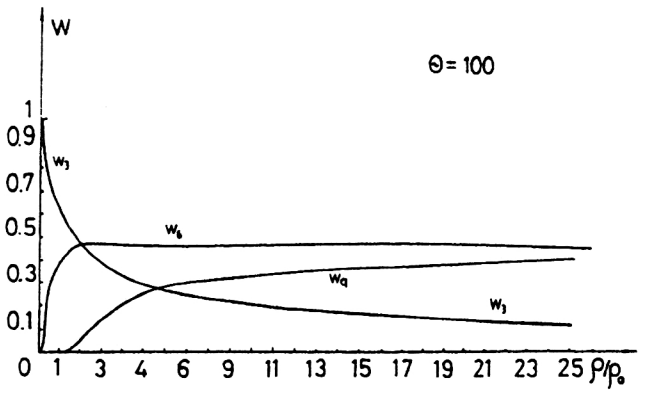

FIG. 9. Cluster probabilities at $\Theta=100$ MeV.

$\rho_q^{\rm nuc}$ may be called the *nucleation density*. As we see, the value of the latter agrees with the corresponding estimates from the Introduction.

The stability of the quark–baryon mixture is controlled by checking the minimum of the free energy $F=\Omega+\Sigma_i\mu_i N_i$, whose density can be written as

$$f\equiv\frac{F}{V}=\frac{\Omega}{V}+\sum_i \mu_i\rho_i=-p+\mu\rho,$$

and also by requiring the validity of the stability conditions[54]

$$-\Theta\frac{\partial^2 f}{\partial\Theta^2}>0, \quad \rho\frac{\partial p}{\partial\rho}>0.$$

The probability of unbound quarks increases with temperature or density monotonically, showing that the deconfinement is a gradual crossover and not a sharp transition. This is in agreement with numerical simulations[121] on a $16^3\times24$ lattice for $N_f=2$, which demonstrated that the quark–quark correlation functions at $\Theta\approx1.5\Theta_d$ are very similar to the zero-temperature wave functions of the corresponding particles.

12. ZERO BARYON DENSITY

The case opposite to that of the previous section is that in which the baryon density is zero, $n_{0B}=0$, and all the particles are generated from the vacuum. Then $\mu_i=0$. In this case, we can compare our calculations with the lattice numerical simulations that are available only for $n_B=0$.

The spectra of gluons and quarks are again taken in the form

$$\omega_g(k)=k+\frac{B}{\rho}, \quad \omega_q(k)=\sqrt{k^2+m_q^2}+\frac{B}{\rho} \tag{51}$$

with the bag-motivated mean fields. The interaction of hadrons is considered in the excluded-volume approximation. The cluster volumes $v_i=m_i v_2/m_2$, according to (45), are expressed in terms of the volume $v_2\equiv4\pi r_2^3/3$ of the lightest cluster with $z_i=2$. The bag constants for the $SU(2)$ and $SU(3)$ systems are different,[122] with the relation $B_{SU(2)}\approx0.4B_{SU(3)}$.

The presentation of results is convenient to perform in relative quantities reduced to those of a reference system. The role of such a system is naturally played by the Stefan–Boltzmann quark–gluon gas. The latter, by definition, is an ensemble of free massless quarks, antiquarks, and gluons. The pressure and energy density of the Stefan–Boltzmann quark–gluon plasma are, respectively,

$$p_{\rm SB}=p_q^{(0)}+p_{\bar q}^{(0)}+p_g^{(0)}, \quad \varepsilon_{\rm SB}=\varepsilon_q^{(0)}+\varepsilon_{\bar q}^{(0)}+\varepsilon_g^{(0)}, \tag{52}$$

where

$$p_i^{(0)}=\pm\Theta\zeta_i\int \ln[1\pm n_i^{(0)}(k)]\frac{d\mathbf{k}}{(2\pi)^3},$$

$$\varepsilon_i^{(0)}=\zeta_i\int kn_i^{(0)}(k)\frac{d\mathbf{k}}{(2\pi)^3}, \tag{53}$$

in which the index $i=q,\bar q,g$ labels quarks, antiquarks, and gluons with the momentum distribution

$$n_i^{(0)}(k)=\{\exp[\beta(k-\mu_i)]\mp1\}^{-1}, \tag{54}$$

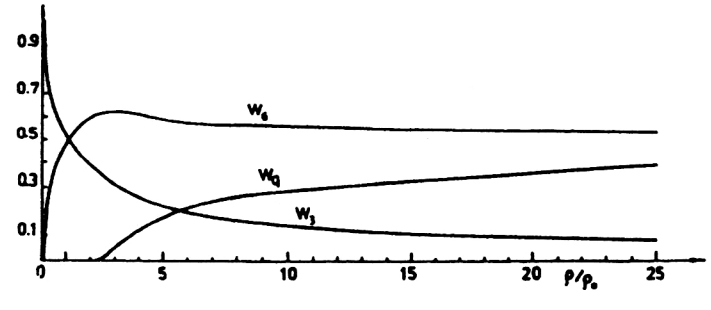

FIG. 8. Cluster probabilities vs relative density at $\Theta=50$ MeV.

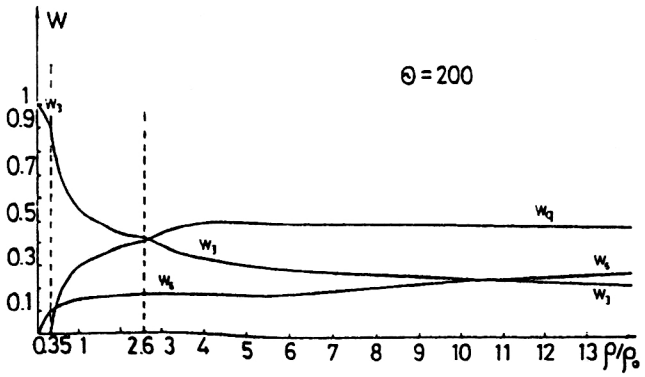

FIG. 10. Cluster probabilities at $\Theta=200$ MeV. Dashed lines show the points of first-order phase transitions. Between these points the matter is a stratified gas–liquid mixture.

with the upper sign for bosons (gluons) and the lower one for fermions (quarks and antiquarks); the chemical potentials are

$$\mu_q=-\mu_{\bar{q}}\equiv\mu, \quad \mu_g=0. \tag{55}$$

Equations (54) and (55) permit us to write (53) as

$$p_i^{(0)}=\frac{\zeta_i}{6\pi^2}\int_0^\infty \frac{k^3dk}{\exp[\beta(k-\mu_i)]\mp 1}, \quad \varepsilon_i^{(0)}=3p_i^{(0)}. \tag{56}$$

An exact integration yields

$$p_q^{(0)}+p_{\bar{q}}^{(0)}=\frac{\zeta_q}{12}\left(\frac{7\pi^2}{30}\Theta^4+\mu^2\Theta^2+\frac{\mu^4}{2\pi^2}\right),$$

$$p_g^{(0)}=\frac{\pi^2}{90}\zeta_g\Theta^4. \tag{57}$$

Thus, the Stefan–Boltzmann pressure is

$$p_{SB}=\frac{\pi^2}{90}\left(\zeta_g+\frac{7}{4}\zeta_q\right)\Theta^4+\frac{\zeta_q}{12}\mu^2\Theta^2\left(1+\frac{\mu^2}{2\pi^2\Theta^2}\right). \tag{58}$$

This is to be compared with the QCD pressure corresponding to the QCD grand potential, given in Sec. 3, for zero coupling $g=0$,

$$p_{QCD}=\frac{\pi^2}{45}\left(N_c^2-1+\frac{7}{4}N_fN_c\right)\Theta^4+\frac{N_fN_c}{6}\mu^2\Theta^2\left(1\right.$$

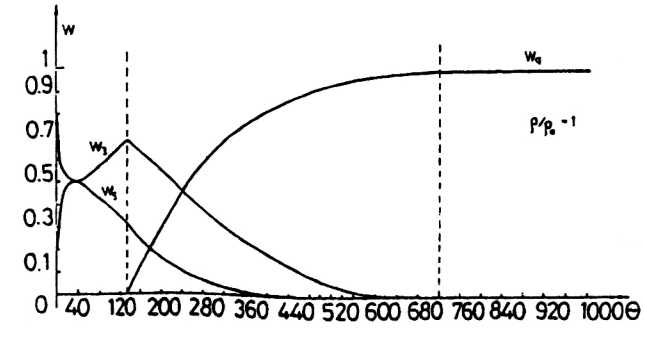

FIG. 11. Nucleon, $6q$-cluster, and quark probabilities as functions of temperature in MeV at the normal density $\rho=\rho_0$.

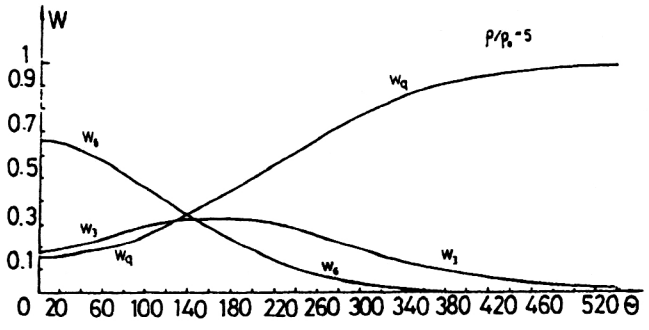

FIG. 12. Cluster probabilities vs temperature at the fixed density $\rho=5\rho_0$.

$$\left.+\frac{\mu^2}{2\pi^2\Theta^2}\right). \tag{59}$$

As a result of the relations for the degeneracy factors of gluons, $\zeta_g=2\times(N_c^2-1)$, quarks, $\zeta_q=2\times N_f\times N_c$, and antiquarks, $\zeta_q=\zeta_{\bar{q}}$, we see that (58) and (59) coincide. Therefore, the Stefan–Boltzmann plasma is the asymptotic high-temperature limit of quantum chromodynamics.

The baryon density for the Stefan–Boltzmann plasma is

$$n_B\equiv\frac{1}{3}(\rho_q-\rho_{\bar{q}})=\frac{\zeta_q}{3}\int[n_q(k)-n_{\bar{q}}(k)]\frac{d\mathbf{k}}{(2\pi)^3}. \tag{60}$$

Either calculating (60) directly or using the derivative $n_B=\partial p/\partial\mu_B$ with $\mu_B=3\mu$, we have

$$n_B=\zeta_q\frac{\mu}{18\pi^2}(\mu^2+\pi^2\Theta^2). \tag{61}$$

From this one gets the equation

$$\mu^3+\pi^2\Theta^2\mu-\frac{18\pi^2}{\zeta_q}n_B=0 \tag{62}$$

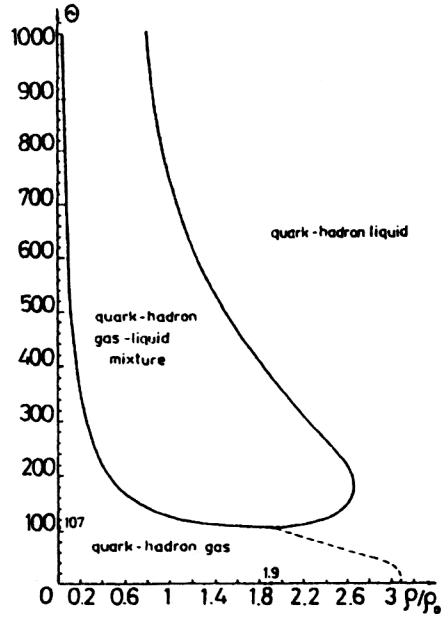

FIG. 13. Phase portrait for baryon-rich quark–hadron matter. Along the dashed line the compressibility is divergent.

TABLE II. Glueball parameters.

Mass m_i (MeV)	Compositeness number z_i	Degeneracy factor ζ_i
960	2	6
1290	2	6
1590	2	6
1460	3	11
1800	3	39

defining $\mu=\mu(n_B)$. At zero baryon density, $n_B=0$, as is clear from (62), one has $\mu=0$.

When the chemical potential is zero, the density of quarks becomes

$$\rho_q=\zeta_q \frac{3\Theta^3}{4\pi^2}\zeta(3) \quad (\mu=0), \tag{63}$$

where $\zeta(3)=1.20206$. For gluons, the chemical potential is always zero, so that their density is

$$\rho_g=\zeta_g \frac{\Theta^3}{\pi^2}\zeta(3). \tag{64}$$

Finally, for the specific heat of the Stefan–Boltzmann plasma we find

$$C_{\rm SB}\equiv\frac{\partial\varepsilon_{\rm SB}}{\partial\Theta}=\frac{2\pi^2}{15}\left(\zeta_g+\frac{7}{4}\zeta_q\right)\Theta^3 + \frac{1}{2}\zeta_q\mu^2\Theta^2\frac{\mu^2-\pi^2\Theta^2}{3\mu^2+\pi^2\Theta^2}. \tag{65}$$

The results of numerical calculations[123–125] for the mixed system consisting of the quark–gluon plasma with the spectrum (51) and of hadrons in the excluded-volume approximation will be presented below for three different situations.

12.1. *SU*(2) quarkless system

The system consists of unbound gluons and of glueballs that are bound gluon clusters. The experimental status of glueballs is as yet uncertain, though there are suggestions[126,127] to interpret a narrow resonance appearing in proton–proton collisions as a scalar glueball. Pure gluodynamics is often studied because it is easier than the full chromodynamics for Monte Carlo lattice simulations.

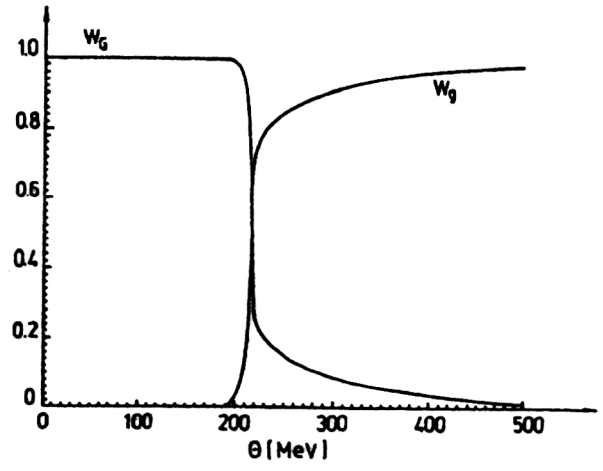

FIG. 15. Comparison of glueball and gluon probabilities for the $SU(2)$ quarkless system.

Glueball masses have been computed in lattice gauge theory for $SU(2)$ (Refs. 43 and 46) as well as for $SU(3)$ (Refs. 128–130) cases. The lattice results are close to the bag-model calculations.[131–133] Here we adopt the glueball masses found in the bag-model approach.[132,133] The corresponding glueball characteristics are given in Table II. The radius r_2 of the lightest glueball with $m_2=960$ MeV is a fitted parameter, which is taken as $r_2=1.2$ fm. The constant B in (51) is chosen to be $B=(165\ \text{MeV})^4$. The gluon degeneracy factor is $\zeta_g=6$ for the $SU(2)$ case.

The results of our calculations are displayed in Figs. 14–18, where the glueball probability w_G and the gluon probability w_g are defined by

$$w_G\equiv\sum_i^{\text{glueballs}} z_i\frac{\rho_i}{\rho}, \quad w_g\equiv\frac{\rho_g}{\rho}=1-w_G.$$

The relative energy density is compared with the lattice data.[134,135] The reference Stefan–Boltzmann plasma here corresponds also to the quarkless case, $N_f=0$. Deconfine-

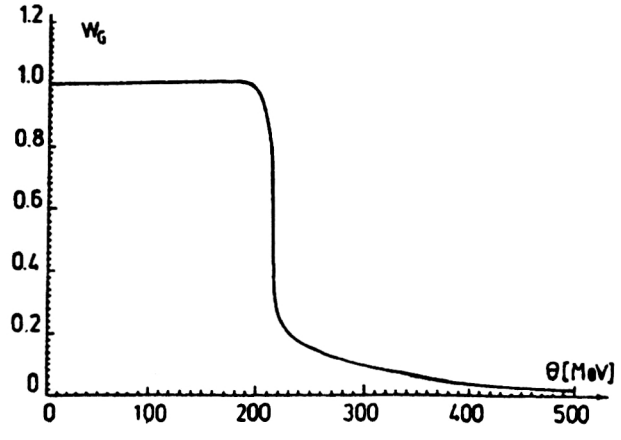

FIG. 14. Glueball probability for the $SU(2)$ quarkless system as a function of temperature.

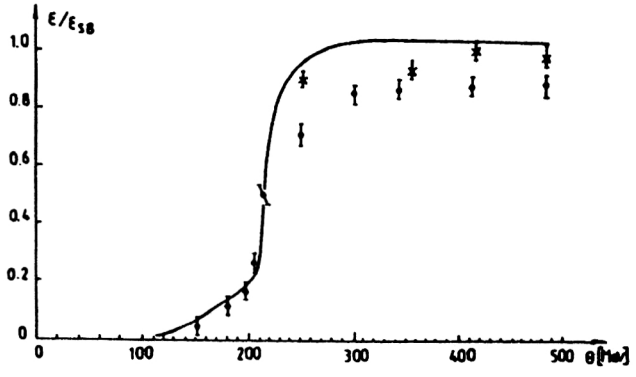

FIG. 16. Relative energy density for the $SU(2)$ quarkless system (solid line) as compared with the lattice Monte Carlo data (Engels *et al.*, 1981).

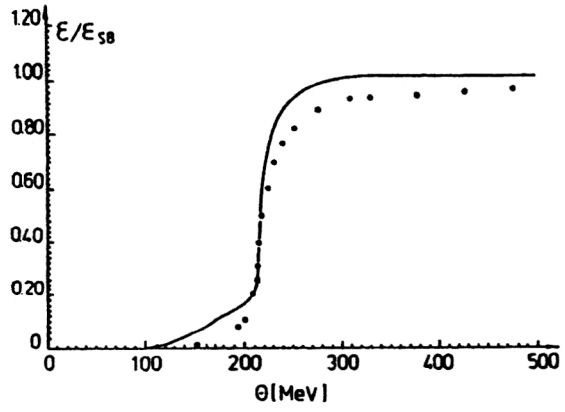

FIG. 17. Relative energy density for the $SU(2)$ quarkless system (solid line) as compared with the lattice numerical simulations (Engels *et al.*, 1989).

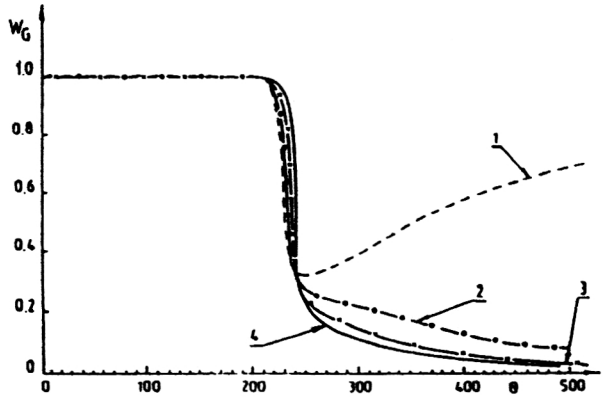

FIG. 19. Glueball probability for the $SU(3)$ quarkless system at several values of the lightest-glueball radius: (1) $r_2=0$; (2) $r_2=0.5$ fm; (3) $r_2=0.7$ fm; (4) $r_2=0.8$ fm.

ment occurs at $\Theta_d=215$ MeV as a second-order transition, which is in agreement with the lattice simulations.

12.2. $SU(3)$ quarkless system

The glueball parameters are taken from Table II. The constant B in the spectra (51) is $B=(235\ \text{MeV})^4$. The gluon degeneracy factor for the $SU(3)$ case is $\zeta_g=16$.

Varying the radius r_2 of the lightest glueball, we have three possibilities: (i) $r_2<r_c$, where $r_c=0.8$ fm; then deconfinement is a gradual crossover. (ii) $r_2=r_c$; in this case deconfinement is a second-order transition. (iii) $r_2>r_c$; then a first-order transition occurs. These possibilities are illustrated in Figs. 19–23, where the entropy density at $\mu_i=0$ is $s=\beta(\varepsilon+p)$ and the reference Stefan–Boltzmann entropy density is $s_{\rm SB}=\beta(\varepsilon_{\rm SB}+p_{\rm SB})=4\beta p_{\rm SB}$. The relative entropy density is compared with the lattice numerical simulations.[136] The latter agrees with our results if $r_2>r_c$, so that deconfinement becomes a first-order transition at about $\Theta_d=230$ MeV.

We emphasize the importance of taking into consideration glueball interactions: When these are absent, that is, $r_2=0$, the behavior of the system is unphysical.

12.3. $SU(3)$ system with quarks

The constituents of the system are taken as follows. We consider quarks of two flavors, $q=\{u,d\}$, and the corresponding antiquarks $\bar{q}=\{\bar{u},\bar{d}\}$ with masses $m_q=m_{\bar{q}}=7$ MeV. The degeneracy factor for each pair of up and down quarks is $\zeta_q=2\times N_f\times N_c=12$, and the same for antiquarks, $\zeta_{\bar{q}}=12$. Gluons have the degeneracy factor $\zeta_g=2\times(N_c^2-1)=16$. From the long list of the known hadrons, we include only those with the lightest masses, which mainly contribute to thermodynamics. These are unflavored mesons (Table III), strange mesons (Table IV), and light baryons (Table V).

For the radius of the lightest hadron, the pion, we take $r_2=r_\pi=0.56$ fm. The radii of all other clusters are expressed in terms of r_π using (45). For the mean-field parameter in (51), we take $B^{1/4}=210$ MeV. The results of calculations are shown in Figs. 24–26, where the hadron cluster probability is defined as

$$w_c\equiv\sum_i^{\text{clusters}} z_i\frac{\rho_i}{\rho}.$$

Deconfinement is found to be a continuous crossover-like transition at $\Theta_d=166$ MeV, which is close to the lattice data.[137]

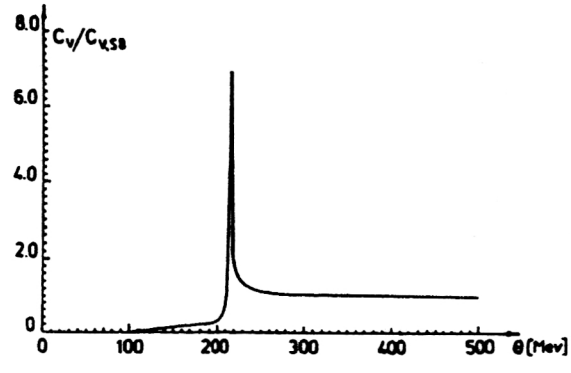

FIG. 18. Reduced specific heat for the $SU(2)$ gluon–glueball mixture. At the deconfinement temperature, the specific heat diverges.

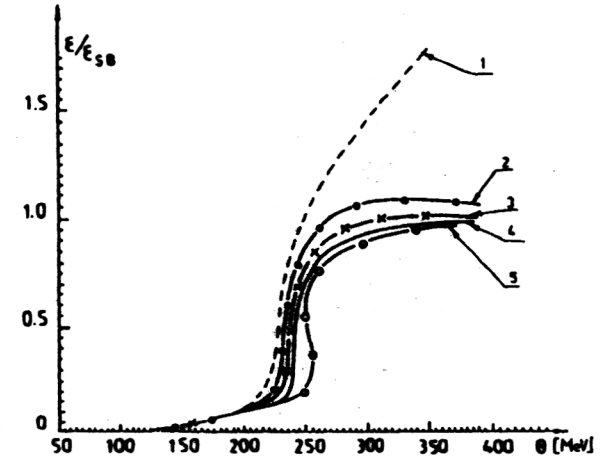

FIG. 20. Relative energy density for the $SU(3)$ quarkless system at: (1) $r_2=0$; (2) $r_2=0.5$ fm; (3) $r_2=0.7$ fm; (4) $r_2=0.8$ fm; (5) $r_2=1$ fm.

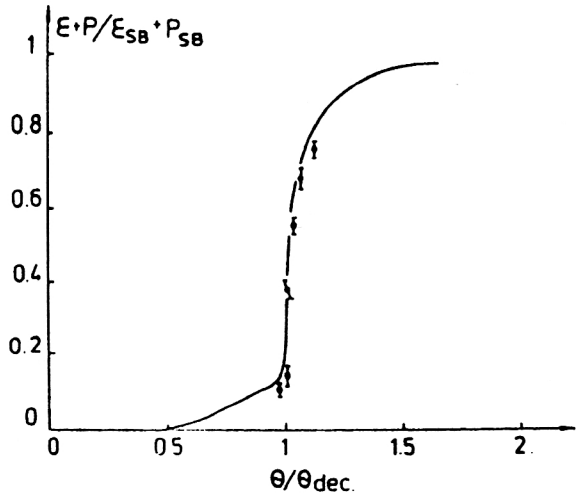

FIG. 21. Relative entropy density for the $SU(3)$ quarkless system at r_2=0.82 fm, compared with the lattice numerical data (Brown *et al.*, 1988).

13. THERMODYNAMIC RESTRICTION RULE

Invoking some approximation, one gets an effective thermodynamic potential, for instance, an effective grand potential $\Omega=\Omega(\Theta,V,\mu,\varphi)$ involving auxiliary functions $\varphi=\{\varphi_j\}$ depending on thermodynamic parameters, the temperature Θ, the volume V, and a set $\mu=\{\mu_i\}$ of chemical potentials. Thus, the effective spectra in (51) contain the mean field $\varphi\equiv B/\rho$. In the excluded-volume approximation, the free volume of the system is factored with the quantity $\xi=1-\Sigma_i\rho_i v_i$, as can be seen from (42). Both ρ and ρ_i are functions of Θ, V, μ. In the cut-off model of Sec. 5, the effective cut-off momentum k_0 is a function of Θ.

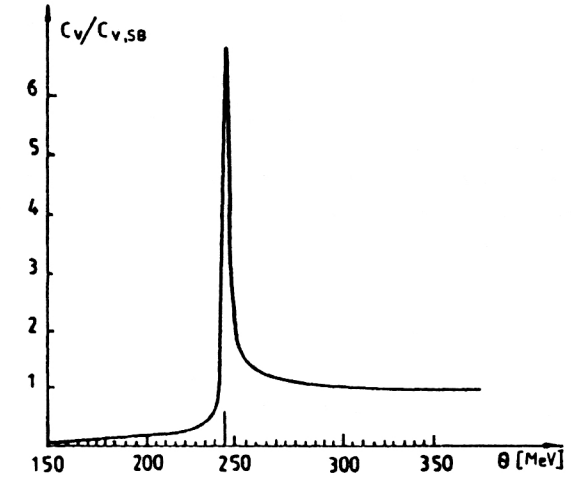

FIG. 22. Reduced specific heat for the $SU(3)$ gluon–glueball mixture at r_2=0.8 fm.

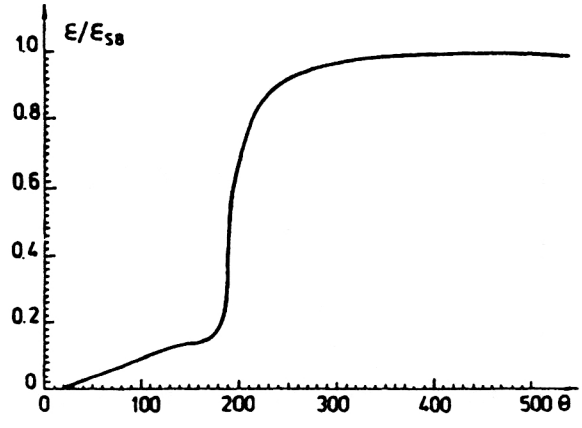

FIG. 23. Relative energy density for the $SU(3)$ quarkless system at $B^{1/4}$=210 MeV and r_2=0.6 fm.

TABLE III. Unflavored meson parameters.

Mesons	Mass m_i (MeV)	Compositeness number z_i	Degeneracy factor ζ_i
π^+	140	2	1
π^-	140	2	1
π^0	135	2	1
η	548	2	1
ρ^+	770	2	3
ρ^-	770	2	3
ρ^0	770	2	3
ω	782	2	3

Effective thermodynamic potentials must be handled with great caution. In fact, if one calculates, e.g., the pressure

$$p=-\frac{\partial\Omega}{\partial V}=-\frac{\Omega}{V}=\frac{\Theta}{V}\ln \mathrm{Tr}\, e^{-\beta H} \tag{66}$$

in two different ways, as the derivative $(-\partial\Omega/\partial V)$ or as the ratio $(-\Omega/V)$, then the answers can be different when Ω includes auxiliary functions depending on V. This would mean that the relation (66) breaks down. The same concerns the energy density, entropy density, and cluster densities, respectively,

$$\varepsilon=\Theta\frac{\partial p}{\partial\Theta}-p+\sum_i \mu_i\rho_i=\frac{1}{V}\langle\hat{E}\rangle,$$

$$s=\frac{\partial p}{\partial\Theta}=\beta\left(\varepsilon+p-\sum_i \mu_i\rho_i\right),$$

$$\rho_i=\frac{\partial p}{\partial\mu_i}=\frac{1}{V}\langle\hat{N}_i\rangle, \tag{67}$$

which can be defined in two ways, as first derivatives of the pressure or as the corresponding statistical averages. The definition (67) can also break down when auxiliary functions depend on thermodynamic variables. This kind of inconsistency occurs as well for the second derivatives, such as the specific heat

TABLE IV. Strange-meson parameters.

Mesons	Mass m_i (MeV)	Compositeness number z_i	Degeneracy factor ζ_i
K^+	494	2	1
K^-	494	2	1
K^0	498	2	2
$\bar{K}^0$	498	2	2

TABLE V. Baryon parameters.

Baryons	Mass m_i (MeV)	Compositeness number z_i	Degeneracy factor ζ_i
N	939	3	4
$\bar{N}$	939	3	4
Δ	1232	3	16
$\bar{\Delta}$	1232	3	16

$$C_V=\frac{\partial\varepsilon}{\partial\Theta}=\frac{\beta^2}{V}\left(\langle\hat{E}^2\rangle-\langle\hat{E}\rangle^2\right) \tag{68}$$

or the isothermic compressibility

$$\kappa_T=-\frac{1}{V}\left(\frac{\partial p}{\partial V}\right)^{-1}=\frac{\beta}{\rho^2 V}\left(\langle\hat{N}^2\rangle-\langle\hat{N}\rangle^2\right). \tag{69}$$

These inconsistencies in defining thermodynamic characteristics in two ways, thermodynamic or statistical, are of course not pleasant. Moreover, the difference between these two ways is not only quantitative, but can also become drastic, especially for systems with phase transitions. It is even possible to give examples when the definition in terms of derivatives yields unphysical divergences in the energy and entropy densities at the phase-transition point. This happens, for instance, as is easy to check, for a pure gluon model in the effective-spectrum approximation.

The simplest procedure for avoiding such troubles can be formulated as follows. Let x be any of the thermodynamic variables Θ, V, or μ. If Ω is an effective grand potential including auxiliary functions depending on these thermodynamic variables, then

$$\frac{\partial\Omega}{\partial x}=\left(\frac{\partial\Omega}{\partial x}\right)_{\varphi}+\frac{\partial\Omega}{\partial\varphi}\cdot\frac{\partial\varphi}{\partial x}.$$

It is just the second term here which causes all the unpleasant problems. Thus, the decision is evident: the derivatives $\partial\Omega/\partial x$ are to be understood in the restricted sense as

$$\frac{\partial\Omega}{\partial x}\to\left(\frac{\partial\Omega}{\partial x}\right)_{\varphi}. \tag{70}$$

The rule (70) may be called the *thermodynamic restriction rule*. We always employ this rule when dealing with effective thermodynamic potentials. If the derivatives in (66)–(69) are understood in the sense of (70), then both ways of calculating thermodynamic characteristics yield the same answers.

Although with the restriction rule (70) we avoid the appearance of spurious terms, so that all the relations (66)–(69) become self-consistent, another problem can arise when dealing with effective thermodynamic potentials. This is the occurrence of instability regions around a transition point, where either the specific heat C_V or the isothermic compressibility κ_T is negative. Below, we illustrate this for the $SU(3)$ quarkless system of Sec. 12.2 with the mean-field parameter $B=(225\ \text{MeV})^4$. The results are shown in Figs. 27–34. The unstable solutions appearing in the vicinity of transition points are related to the loss of convexity of the pressure. To restore the convexity, we may resort to the Maxwell construction of smoothing the corresponding thermodynamic potential.[138] Such a smoothing is shown in Figs. 31 and 32. The behavior of the resulting pressure and energy density is in reasonable agreement with lattice simulations.[50] Nevertheless, a slight dissatisfaction remains in the fact that instability regions occur not only around a first-order transition, where this would be more or less natural, but also in the vicinity of a continuous transition.

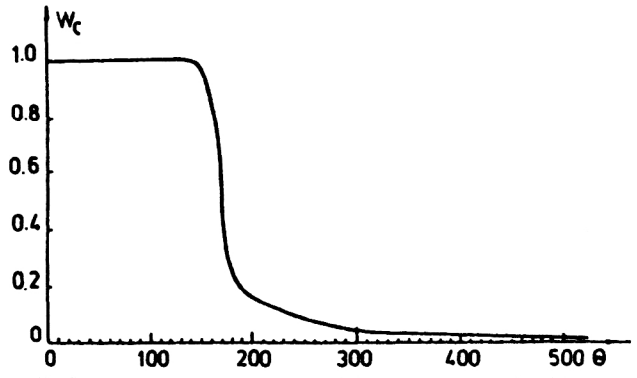

FIG. 24. Hadron cluster probability for the mixture of quark–gluon plasma and hadrons at zero baryon density.

Instead of relying on the restriction rule (70), it would seem rational to define an effective thermodynamic potential from the beginning in such a way that all the necessary thermodynamic relations are automatically valid. This goal can be achieved[139] by redefining the thermodynamic characteristics with the help of shifts of the chemical potentials, $\mu_i\to\mu_i-u_i$, pressure, $p\to p+p'$, energy density, $\varepsilon\to\varepsilon+\varepsilon'$, and entropy density, $s\to s+s'$, requiring that the shifting functions u_i, p', ε', and s' guarantee the validity of (66) and (67). The latter are then called self-consistency conditions.[139] In this case, (66) and (67) constitute a system of nonlinear differential equations for the functions u_i, p', ε', and s', in partial derivatives with respect to the variables Θ, V, and μ_i. Such a system has no unique solution, especially when no boundary conditions are known. To extract a solution from the self-consistency equations we need several additional heuristic assumptions and fitting parameters. Some simplification comes from the guideline prescribed by mean-field approximations.[140–142]

14. PRINCIPLE OF STATISTICAL CORRECTNESS

In this section we present a new principle allowing a correct construction of effective thermodynamic potentials. This principle, as compared to the self-consistency conditions, is: (i) more general, yielding these conditions, but not conversely; (ii) much simpler to deal with; (iii) unambiguous, providing a unique solution.

Let an effective thermodynamic potential $\Omega_{\text{eff}}=\Omega_{\text{eff}}(\varphi)$ include a set $\varphi=\{\varphi_i(x)\}$ of auxiliary functions depending on arbitrary variables x. The latter, in particular, may incorporate space and thermodynamic variables. First of all, it is necessary to understand that not any effective potential can make sense, however reasonable it may look. Each thermodynamic potential, to be accepted as such, must have the properties formulated below.

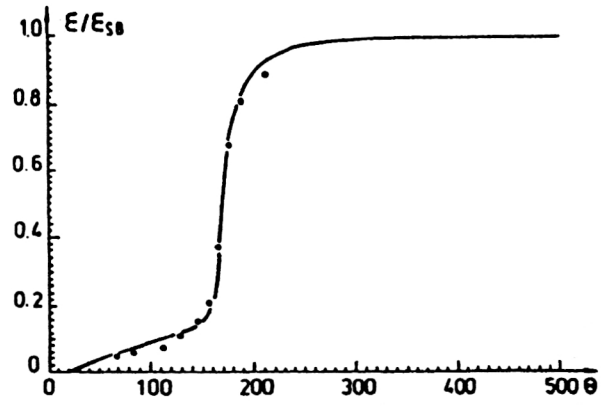

FIG. 25. Relative energy density for the mixture, compared with the lattice numerical calculations (Çelik *et al.*, 1985).

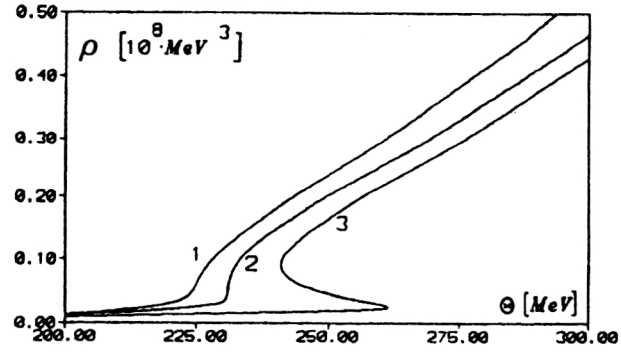

FIG. 27. Total density as a function of temperature for the $SU(3)$ gluon–glueball mixture at different values of the lightest-glueball radius: (1) $r_2=0.6$ fm; (2) $r_2=0.8$ fm; (3) $r_2=1$ fm.

Property 1. **Statistical Representability:**

An effective thermodynamic potential Ω_{eff} represents an equilibrium statistical system if and only if it has the Gibbs form

$$\Omega_{\text{eff}}(\varphi)=\Omega[H_{\text{eff}}(\varphi)], \tag{71}$$

where

$$\Omega[H]\equiv-\Theta \ln \mathrm{Tr}\, e^{-\beta H}, \tag{72}$$

depending on auxiliary functions only through an effective Hamiltonian $H_{\text{eff}}=H_{\text{eff}}(\varphi)$. Such a thermodynamic potential is called *statistically representable.*

In this way, if one invents an effective thermodynamic potential, even pronouncing seemingly plausible words, this does not mean that the invented potential describes some statistical system. If the potential is not statistically representable, it represents no equilibrium statistical system. For example, a thermodynamic potential in the excluded-volume approximation is not statistically representable. Although the latter approximation may occasionally give a reasonable description, in general it is not trustworthy. The excluded-volume approximation may be used, because of its simplicity, as a first attempt at understanding the qualitative behavior of a system, but it should be always followed by a more reliable approximation.

Property 2. **Thermodynamic Equivalence:**

A statistical system described by a given Hamiltonian H_{giv} is thermodynamically equivalent to a system modeled by an effective Hamiltonian H_{eff} if and only if their thermodynamic potentials are statistically representable,

$$\Omega_{\text{giv}}=\Omega[H_{\text{giv}}], \quad \Omega_{\text{eff}}=\Omega[H_{\text{eff}}], \tag{73}$$

and are equal to each other,

$$\Omega[H_{\text{giv}}]=\Omega[H_{\text{eff}}]. \tag{74}$$

The corresponding Hamiltonians are called *thermodynamically equivalent.*

For the case of infinite matter, such as nuclear matter, the equality (74) can be softened by requiring the validity of the asymptotic (in the thermodynamic limit) equality

$$\lim_{V\to\infty}\frac{1}{V}\left(\Omega[H_{\text{giv}}]-\Omega[H_{\text{eff}}]\right)=0.$$

Property 3. **Statistical Equilibrium:**

The necessary condition for an equilibrium statistical system modeled by an effective Hamiltonian $H_{\text{eff}}(\varphi)$ to be thermodynamically equivalent to a given statistical system with H_{giv} is the equilibrium condition

$$\left\langle\frac{\delta}{\delta\varphi}H_{\text{eff}}(\varphi)\right\rangle=0, \tag{75}$$

where the variation over φ implies a set of variations with respect to each φ_i and

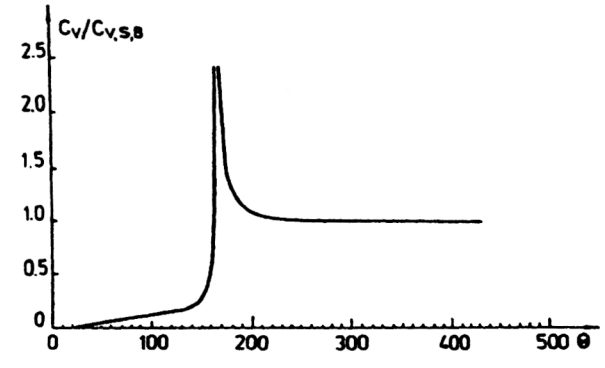

FIG. 26. Reduced specific heat for the mixture of quark–gluon plasma and hadrons at zero baryon density.

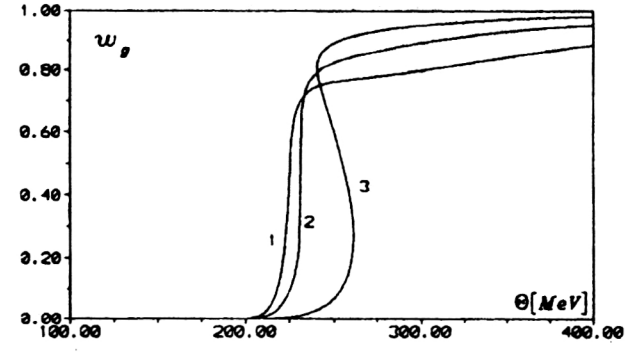

FIG. 28. Gluon probability vs temperature for the values of r_2 as in Fig. 27.

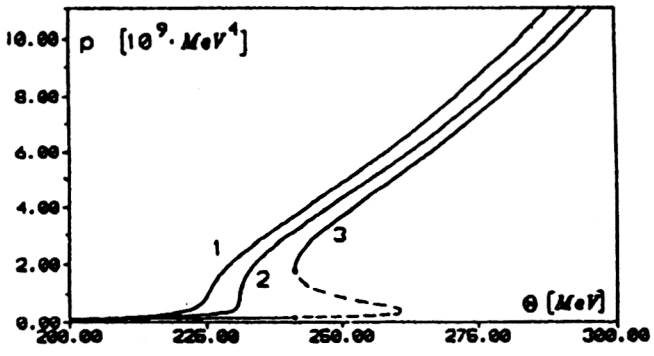

FIG. 29. Pressure of the gluon–glueball mixture vs temperature for the same values of r_2 as in Fig. 27.

$$\langle \hat{A} \rangle \equiv \frac{\mathrm{Tr}\, \hat{A} \exp(-\beta H_{\mathrm{eff}})}{\mathrm{Tr} \exp(-\beta H_{\mathrm{eff}})} .$$

The proof of (75) is straightforward on the basis of statistical representability (71), thermodynamic equivalence (74), and the fact that Ω_{giv} does not depend on φ.

Now we can formulate the central notion:

Principle of Statistical Correctness:

An effective thermodynamic potential is statistically correct if it is statistically representable with an effective Hamiltonian satisfying the condition (75) of statistical equilibrium.

As is evident, the self-consistency conditions for the first-order derivatives (66) and (67) immediately follow from (75). Moreover, the self-consistency conditions for the second-order derivatives (68) and (69) also follow from (75), as well as such conditions for the derivatives of arbitrary order. If one finds the shifting functions from the first-order self-consistency conditions (66) and (67), the second-order conditions (68) and (69) are not necessarily fulfilled.

We shall also say that an effective Hamiltonian is statistically correct if it satisfies (75). The same can be said about an approximation leading to a statistically correct Hamiltonian. For instance, the correlated mean-field approximation of Sec. 9, involving the conditions (26), or (27), or (31), is statistically correct.

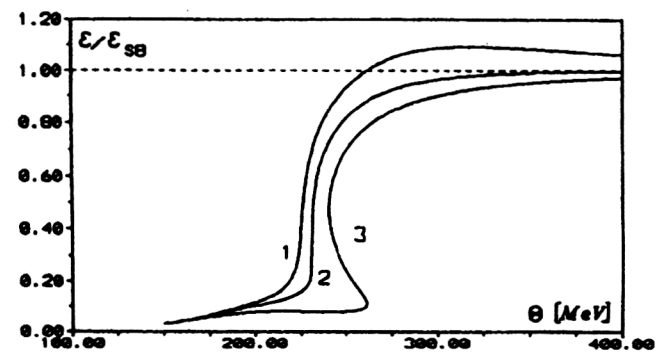

FIG. 30. Relative energy of the mixture for the values of r_2 as in Fig. 27.

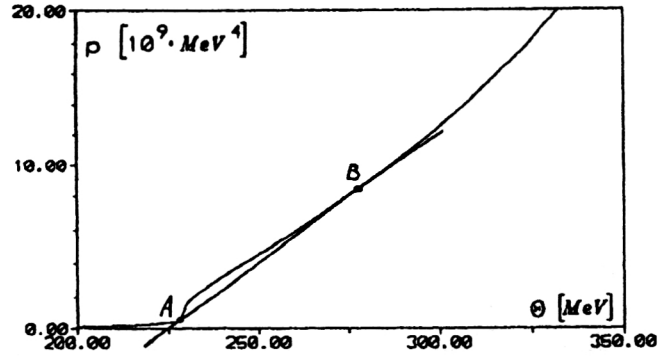

FIG. 31. Smoothing of pressure in the unstable crossover region at r_2=0.7 fm.

15. CLUSTERING QUARK–HADRON MATTER

To obtain a statistically correct description of the quark–gluon plasma clustering into hadron states, let us use the correlated mean-field approximation,[35] leading to the Hamiltonian

$$H = \sum_i H_i + CV,$$

$$H_i = \sum_k \omega_i(k) a_i^{\dagger}(\mathbf{k}) a_i(\mathbf{k}),$$

$$\omega_i(k) = \sqrt{k^2 + m_i^2} + U_i - \mu_i \qquad (76)$$

discussed in Sec. 9.

Consider the case of the conserved baryon number $N_B = \Sigma_i N_i^B$ with $N_i^B \equiv B_i N_i$, where B_i is the baryon number of an i cluster. For an equilibrium system, the relation

$$\mu_i = B_i \mu_B \qquad (77)$$

holds between the chemical potential μ_i and the baryon potential μ_B. The latter may be defined as a function $\mu_B(n_B)$ of the baryon density

$$n_B \equiv \frac{N_B}{V} = \sum_i B_i \rho_i . \qquad (78)$$

The index i labels the constituents. The complete set $\{i\}$ of these indices consists of two different groups, $\{i\} = \{i\}_{\mathrm{pl}} \cup \{i\}_{\mathrm{cl}}$. The first group $\{i\}_{\mathrm{pl}}$ corresponds to the

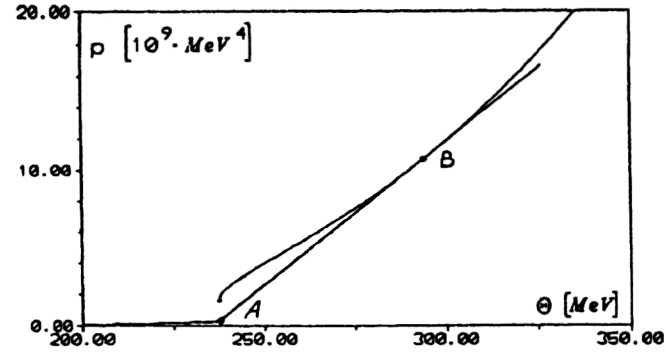

FIG. 32. Smoothing of pressure in the region of the first-order phase transition at r_2=1 fm.

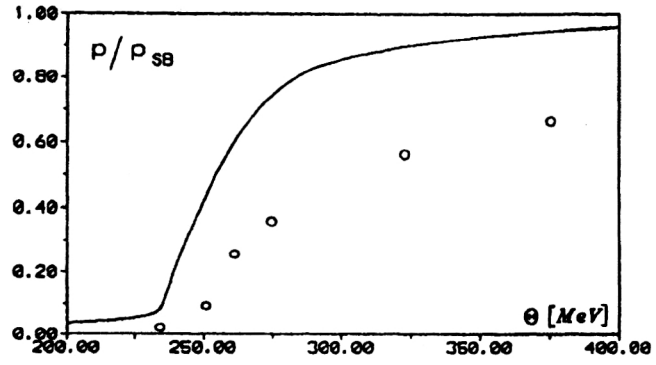

FIG. 33. Relative smoothed pressure for the gluon–glueball system at $r_2=0.9$ fm (solid line) as compared with the lattice simulation data (Engels, 1991).

plasma constituents, quarks, antiquarks, and gluons, which are elementary particles, thus having compositeness number $z_i=1$. The second group $\{i\}_{\rm cl}$ labels hadron clusters that are bound states with compositeness numbers $z_i\geq 2$. Accordingly, the total density of matter

$$\rho=\sum_i z_i\rho_i=\rho_{\rm pl}+\rho_{\rm cl} \tag{79}$$

consists of two terms

$$\rho_{\rm pl}=\sum_{\{i\}_{\rm pl}}\rho_i, \quad \rho_{\rm cl}=\sum_{\{i\}_{\rm cl}} z_i\rho_i,$$

corresponding to the plasma density $\rho_{\rm pl}$ and the cluster density $\rho_{\rm cl}$.

We define the plasma mean fields U_i, when $i\in\{i\}_{\rm pl}$, as

$$U_i=U(\rho)=\rho\int V(r)s(r)d\mathbf{r}, \tag{80}$$

where $V(r)$ is a confining potential and $s(r)$ is a screening function. Before substituting into (80) a concrete confining potential, let us emphasize the general properties which the plasma mean field $U(\rho)$ must satisfy. These properties are

$$U(\rho)\to\infty \quad (\rho\to 0),$$
$$U(\rho)\to 0 \quad (\rho\to\infty). \tag{81}$$

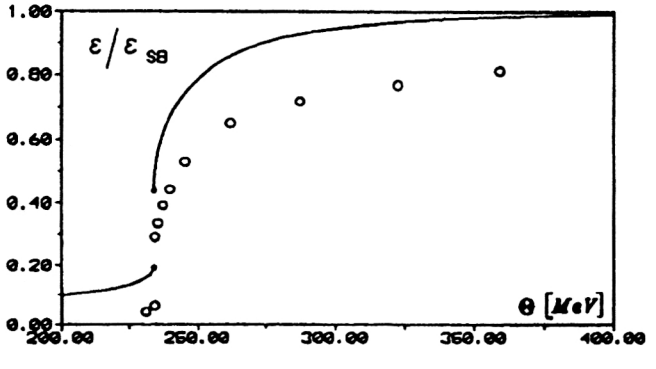

FIG. 34. Relative smoothed energy at $r_2=0.9$ fm (solid line), compared with the lattice data (Engels, 1991).

The first condition in (81) means that quarks and gluons cannot exist as unbound particles at low density, that is, color confinement must occur as $\rho\to 0$. Alternatively, one may say that quarks and gluons cannot exist as free particles outside dense nuclear matter. The second condition in (81) reflects the phenomenon of asymptotic freedom.

There are different types of confining potentials: linear, quadratic, logarithmic, and with noninteger powers. For example, the interaction between a heavy quark and its antiquark is usually taken in the form of the Cornell potential[143,144] with a linear confining term. This form of the potential is confirmed by QCD calculations[145] and by lattice simulations.[146] The quadratic confining potential is also quite popular.[77,80,91] In addition, the strength of the mutual interactions between the three plasma constituents, the quarks, antiquarks, and gluons, is different.[145,147] The confining potential $V(r)$ in (80) is assumed to be an averaged potential of the form

$$V(r)=Ar^\nu \quad (0\leq\nu\leq 2). \tag{82}$$

The screening function $s(r)=c(r/a)$ is usually[91] scaled with the mean interparticle distance $a\equiv\rho^{-1/3}$. Therefore, the plasma mean field (80) with the confining potential (82) can be written as

$$U(\rho)=J^{1+\nu}\rho^{-1/3}, \tag{83}$$

where

$$J^{1+\nu}\equiv 4\pi A\int_0^\infty c(x)x^{2+\nu}dx.$$

We can calculate the constant J if A and $c(x)$ are known. Alternatively, we can treat J as a free parameter. The value of J can be estimated as follows. Suppose that at the normal quark density ρ_0 the plasma mean field (83) becomes

$$U(\rho_0)=3E_0=3\rho_0^{1/3}, \tag{84}$$

where the factor 3 stands for the three plasma constituents. Then from (83) and (84) we obtain

$$J=3^{1/(1+\nu)}\rho_0^{1/3}. \tag{85}$$

Thus, for linear confinement, $\nu=1$, we get $J=272$ MeV, while for quadratic confinement, $\nu=2$, we have $J=226$ MeV.

For the mean field of an i cluster we can write

$$U_i=\sum_{\{j\}_{\rm cl}}\Phi_{ij}\rho_j+z_i[U(\rho)-U(\rho_{\rm cl})], \tag{86}$$

where the first term describes the interaction of the given cluster with other clusters, and the second term corresponds to the interaction of this cluster with the quark–gluon plasma. The interaction potentials between clusters can be scaled according to (20), which permits us to express the interaction integrals (29) in terms of one scaling integral as

$$\Phi_{ij}=z_iz_j\Phi. \tag{87}$$

Allowance for (83) and (87) reduces (86) to

$$U_i=z_i\Phi\rho_{\rm cl}+z_iJ^{1+\nu}(\rho^{-\nu/3}-\rho_{\rm cl}^{-\nu/3}). \tag{88}$$

In the effective Hamiltonian (76) with the mean fields (83) and (88) the role of the auxiliary functions is played by the densities ρ and $\rho_{\rm cl}$. Thus, for the equilibrium conditions (75) we have

$$\left\langle \frac{\partial H}{\partial \rho} \right\rangle = 0, \quad \left\langle \frac{\partial H}{\partial \rho_{\rm cl}} \right\rangle = 0. \tag{89}$$

From (89) we have two variational equations of the type (31), whose solution, apart from a constant, is easy to find:

$$C = \frac{\nu}{3-\nu} J^{1+\nu} (\rho^{1-\nu/3} - \rho_{\rm cl}^{1-\nu/3}) - \frac{1}{2} \Phi \rho_{\rm cl}^2. \tag{90}$$

In this way, the effective Hamiltonian is completely defined, and we can proceed to particular calculations.

15.1. Pure gluon system

Imagine an extreme situation when only gluons can exist. This case can be obtained from the general model by putting all the degeneracy factors equal to zero except that of the gluons, $\zeta_g \neq 0$. Then $\rho = \rho_g$ and $\rho_{\rm cl} = 0$. Employing the Boltzmann approximation, we find[148] that there is a first-order vacuum–gluon-plasma transition at

$$\Theta_d = J \left[\frac{\nu}{3-\nu} \exp\left(1 - \frac{\nu}{3}\right) \left(\frac{\pi^2}{\zeta_g}\right)^{\nu/3} \right]^{1/(1+\nu)}.$$

Below Θ_d there is exactly the vacuum, empty space, with zero energy density, $\varepsilon = 0$. Gluons appear at Θ_d with a jump. The relative latent heat at Θ_d is

$$\frac{\Delta \varepsilon_d}{\varepsilon_{\rm SB}} = \frac{1+\nu}{\nu} \exp\left(1 - \frac{3}{\nu}\right).$$

The degeneracy of the gluons for the $SU(3)$ case is $\zeta = 16$. For linear confinement with $\nu = 1$, we get $\Theta_d = 248$ MeV and $\Delta \varepsilon_d / \varepsilon_{\rm SB} = 0.27$. For harmonic confinement, when $\nu = 2$, the vacuum–gluon transition occurs at a higher temperature $\Theta_d = 285$ MeV and the latent heat is larger, $\Delta \varepsilon_d / \varepsilon_{\rm SB} = 0.91$.

15.2. $SU(2)$ gluon–glueball system

The gluon degeneracy factor for the $SU(2)$ case is $\zeta = 6$. For the scaling integral we take $\Phi = \Phi_{22}/4$. Then the interactions between glueballs are found from (87). We consider the glueballs listed in Table II. There are two fitting parameters, for which we take $J = 175$ MeV and $\Phi_{22} = 38.42$ GeV·fm^3, so that $\Phi = 9.61$ GeV·fm^3. The results of our calculations[148–151] are shown in Figs. 35–37 for quadratic confinement, $\nu \approx 2$. Actually, the results do not change much in the interval $1.5 \leq \nu \leq 2$. We have mainly used $\nu = 1.86$. Deconfinement is a second-order transition at $\Theta_d = 210$ MeV. It can be seen that the agreement with the lattice simulations[135] is excellent.

15.3. $SU(3)$ gluon–glueball mixture

For the gluon degeneracy factor we have $\zeta_g = 16$. The power ν of the confining interaction is, as in the previous subsection, close to quadratic. But the fitting parameters are $J = 225$ MeV and $\Phi = 3.84$ GeV·fm^3. The glueball characteristics are again taken from Table II. Calculations show[148,149] that a first-order transition occurs at $\Theta_d = 225$ MeV with relative latent heat $\Delta \varepsilon_d / \varepsilon_{\rm SB} = 0.23$. The agreement with the Monte Carlo lattice simulations[50,51,152] is also very good (Figs. 38 and 39).

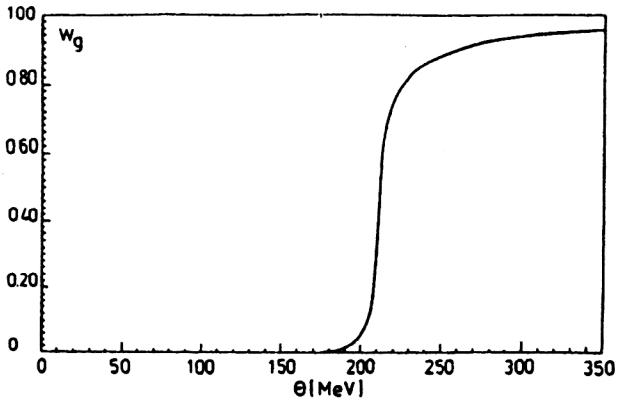

FIG. 35. Gluon probability for the corrected $SU(2)$ quarkless model.

15.4. Mixed quark–gluon–meson system

Consider the case of zero baryon density, $n_B = 0$. Take the quarks of two flavors, u and d, and the related antiquarks, $\bar{u}$ and $\bar{d}$. Assume, for simplicity, that all their masses are equal, $m_u = m_d = 7$ MeV. The degeneracy factor for each kind of quark is $\zeta_u = \zeta_d = 2N_c = 6$. This factor for gluons is $\zeta_g = 16$. Hadrons are represented by mesons from Tables III and IV. Following Sec. 11, we take $\Phi_{33} = 315$ MeV·fm^3, so that $\Phi = \Phi_{33}/9 = 35$ MeV·fm^3. The plasma interaction parameter $J = 225$ MeV is the same as in the previous subsection, as well as $\nu \approx 2$ corresponding to quadratic confinement. Thus, here we do not add any new fitting parameters.

Our calculations[148,149] displayed in Fig. 40 prove that there is no sharp phase transition, but there is a gradual crossover. The deconfinement transition can be attributed to the temperature $\Theta_d = 150$ MeV at which the relative specific heat $C_V / C_{\rm SB}$ has a maximum. The latter is finite and looks more like a Schottky anomaly[153] than a narrow divergent peak typical of a second-order phase transition. The agreement of our results with the lattice-simulation data[137] is again quite good. The lattice results[137] indicate that the deconfinement transition is really continuous. From the point of view

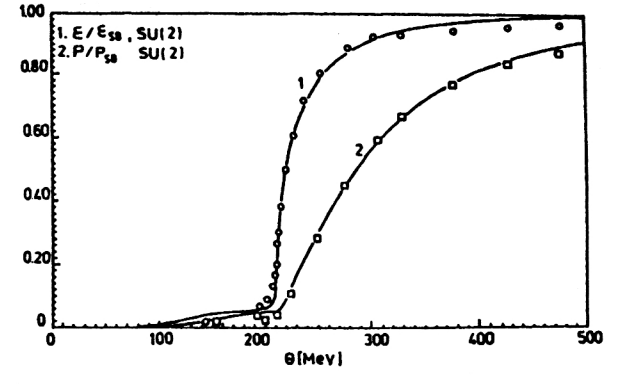

FIG. 36. Relative energy and pressure for the corrected $SU(2)$ gluon–glueball model. Circles and squares are lattice simulation data (Engels, 1989).

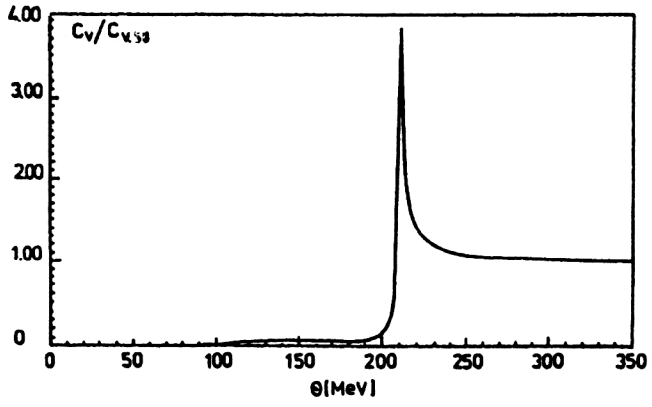

FIG. 37. Reduced specific heat for the corrected $SU(2)$ quarkless model.

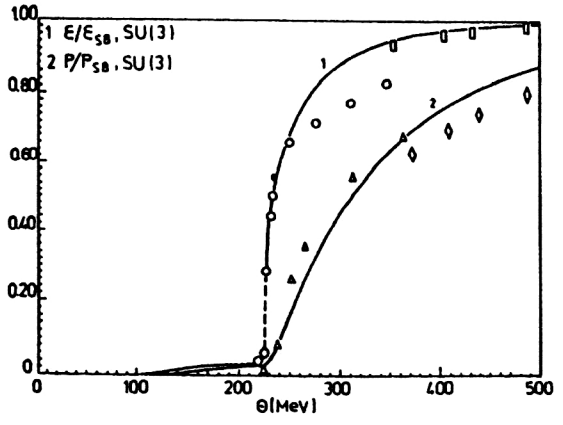

FIG. 39. Relative energy and pressure for the corrected $SU(3)$ quarkless model, compared with lattice Monte Carlo calculations (Brown *et al.*, 1988; Karsch, 1989; Engels, 1991; Petersson, 1991).

of QCD this can be understood as follows. The role of the quark term in the QCD Lagrangian is similar to that of an external magnetic field applied to a spin system. In the presence of a magnetic field, the ferromagnet–paramagnet transition in simple spin systems becomes a continuous crossover.

15.5. Finite baryon density

Here we extend the considerations to nonzero baryon density. The parameters J and Φ are the same as in the previous subsection. Again, we study the two-flavor case with the same characteristics. We take mesons from Table III, protons and neutrons from Table V, and multiquarks from Table I. For a six-quark cluster we take $m_6=1944$ MeV. The Bose–Einstein condensate of six quarks occurs when $\omega_6(0)=0$. Then the baryon potential is

$$\mu_B=\tfrac{1}{2}m_6+3\Phi\rho_{\rm cl}+3J^{1+\nu}(\rho^{-\nu/3}+\rho_{\rm cl}^{-\nu/3}),$$

and the density of six quarks consists of two terms:

$$\rho_6=\frac{\zeta_6}{(2\pi)^3}\int n_6(k)d\mathbf{k}+\rho_6^0.$$

We have analyzed the behavior of several probabilities[154–157] as functions of the temperature Θ and the relative baryon density n_B/n_{0B}. This is demonstrated in Fig. 41 for the plasma probability

$$w_{\rm pl}=\frac{1}{\rho}(\rho_g+\rho_u+\rho_{\bar u}+\rho_d+\rho_{\bar d}),$$

in Fig. 42 for the pion probability

$$w_\pi=\frac{2}{\rho}(\rho_{\pi^+}+\rho_{\pi^-}+\rho_{\pi^0}),$$

in Fig. 43 for the summed (excluding pions) probability of other mesons,

$$w_{\eta\rho\omega}=\frac{2}{\rho}(\rho_\eta+\rho_{\rho^+}+\rho_{\rho^-}+\rho_{\rho^0}+\rho_\omega)\equiv w_{\rm mes},$$

in Fig. 44 for the nucleon probability

$$w_3=\frac{3}{\rho}(\rho_p+\rho_{\bar p}+\rho_n+\rho_{\bar n}),$$

in Fig. 45 for the six-quark probability

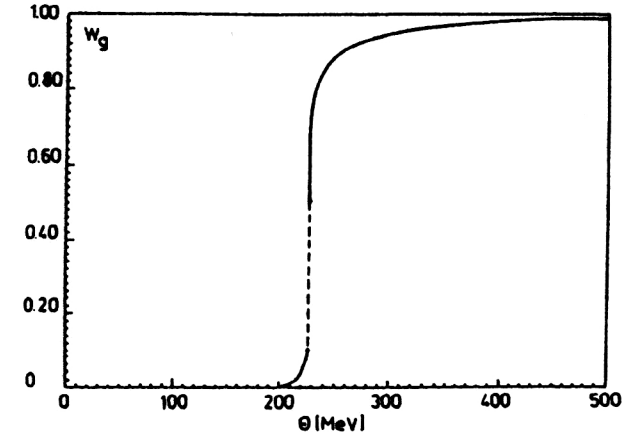

FIG. 38. Gluon probability for the corrected $SU(3)$ gluon–glueball model.

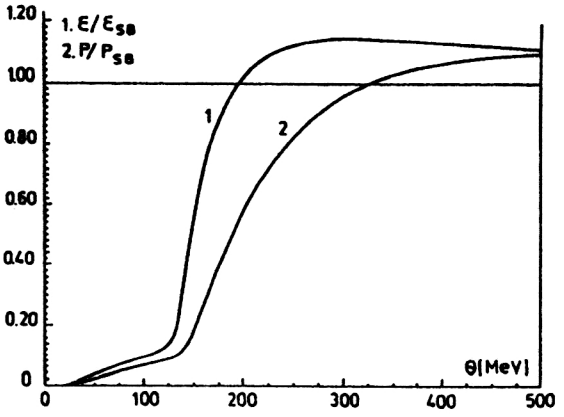

FIG. 40. Relative energy and pressure for the mixed quark–gluon–meson system.

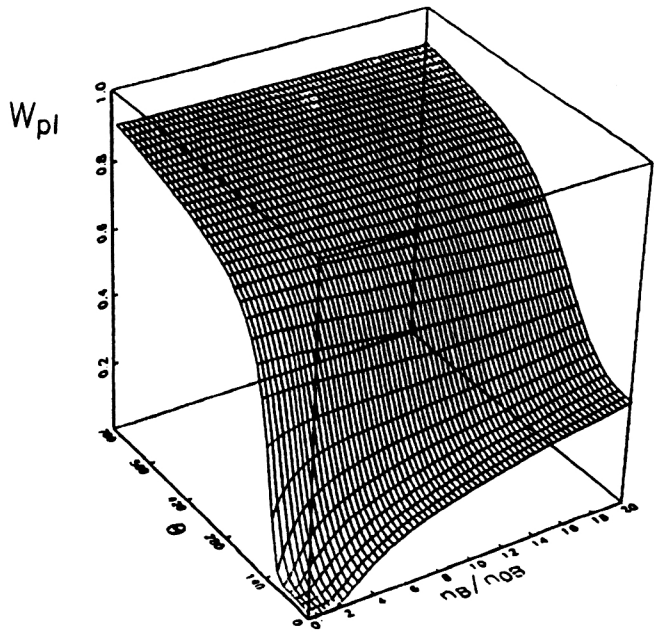

FIG. 41. Quark–gluon plasma probability in the temperature–baryon-density plane.

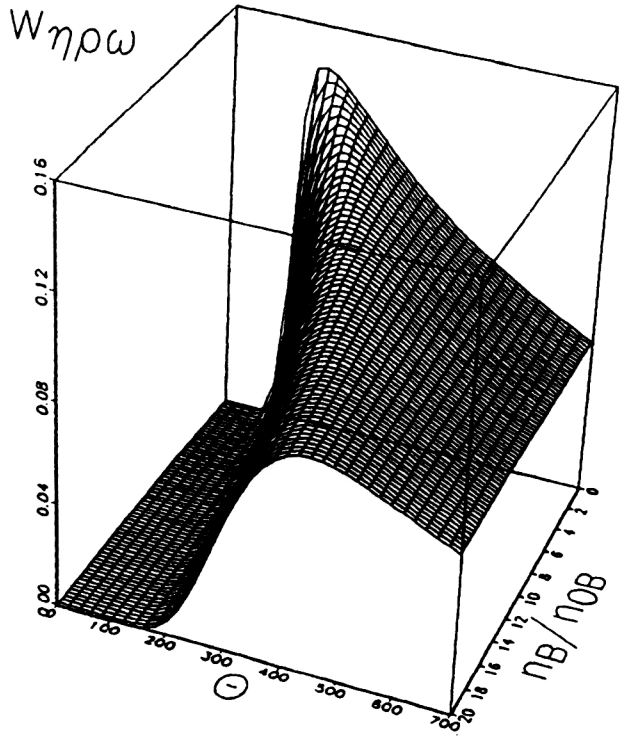

FIG. 43. The total probability of η, ρ, and ω mesons.

$$w_6=\frac{6}{\rho}(\rho_6+\rho_{\bar{6}}),$$

and in Fig. 46 for the probability of condensed six-quark clusters,

$$w_6^0=\frac{6}{\rho}\rho_6^0.$$

In addition, we present here some other thermodynamic characteristics permitting us to understand better the features of the deconfinement transition. The ratio of pressure to energy density, which has the meaning of the effective squared sound velocity

$$c_{\text{eff}}^2=\frac{p}{\varepsilon},$$

is given in Fig. 47. At $n_B=0$ the temperature dependence of c_{eff}^2 agrees with that reconstructed from the lattice data.[158] The reduced specific heat

$$\sigma_V=\frac{\Theta}{\varepsilon}\frac{\partial\varepsilon}{\partial\Theta}$$

and the dimensionless compressibility coefficient

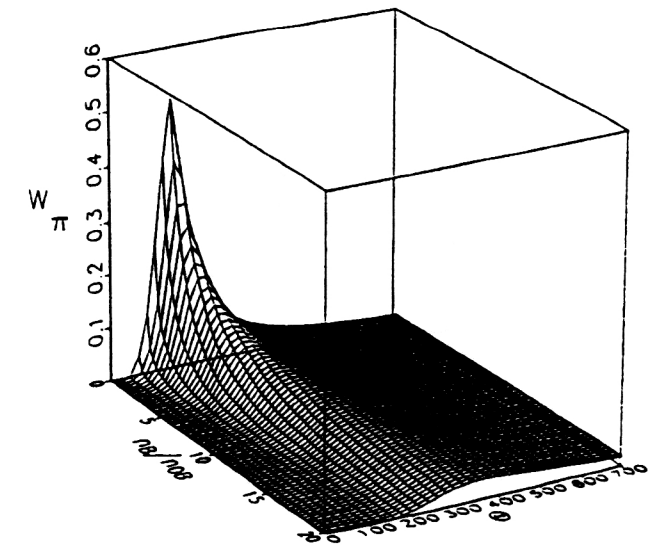

FIG. 42. The probability of π mesons.

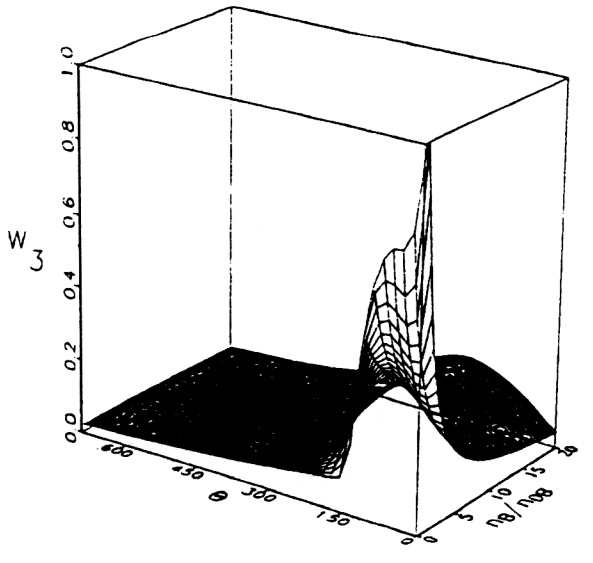

FIG. 44. The nucleon probability.

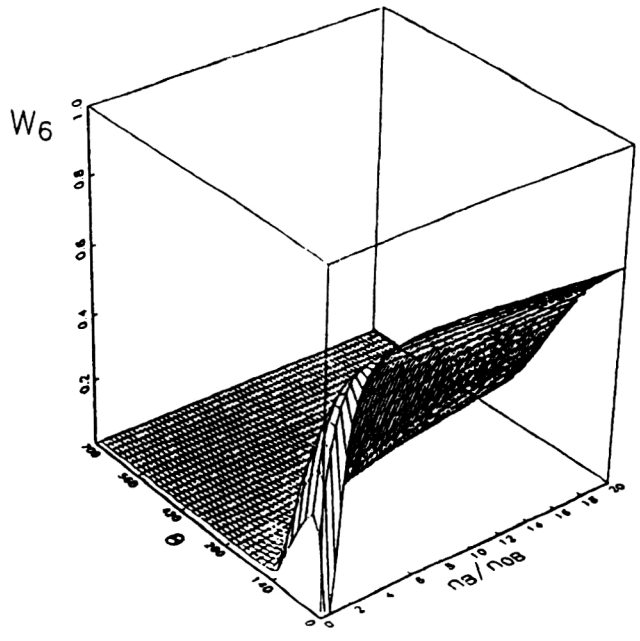

FIG. 45. The probability of six-quark clusters.

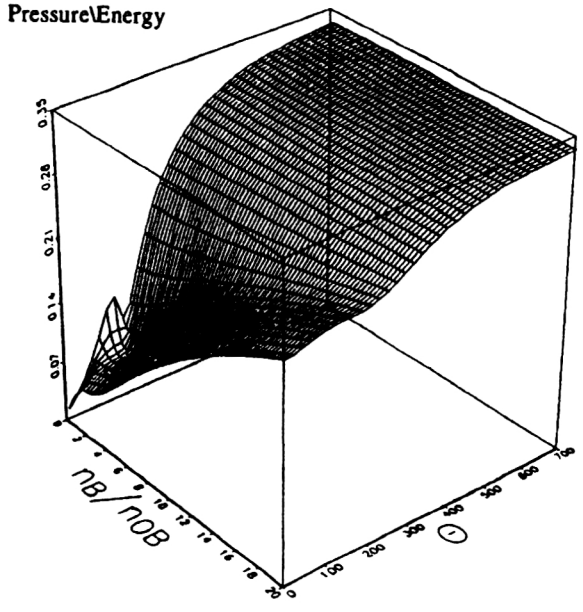

FIG. 47. Pressure-to-energy ratio in the temperature–baryon-density plane.

$$\kappa_T = \left(\frac{n_B}{J^4} \frac{\partial p}{\partial n_B} \right)^{-1}$$

are depicted in Figs. 48 and 49, respectively. The transition line can be ascribed to the maximum of the inverse compressibility coefficient κ_T^{-1}, which can be called[111] the compression modulus (see Fig. 50).

We shall not discuss in detail the peculiarities of the calculated thermodynamic functions because we think that the presented figures already give a good visual demonstration, and also to avoid making this review too long. Let us only emphasize that the deconfinement transition is a continuous crossover, becoming smoother and smoother with increasing baryon density. The deconfinement at a fixed low temperature and rising baryon density is due to the disintegration of hadrons into unbound quarks. When both the temperature and baryon density increase, the deconfinement is a result of the hadron disintegration as well as of the generation from the vacuum of quarks and gluons.

In conclusion, we may state that allowance for the coexistence of hadrons and the quark–gluon plasma is vitally important for constructing a unified approach and is in agreement with the lattice-simulation data. The gradual character of the deconfinement transition, occurring through a mixed

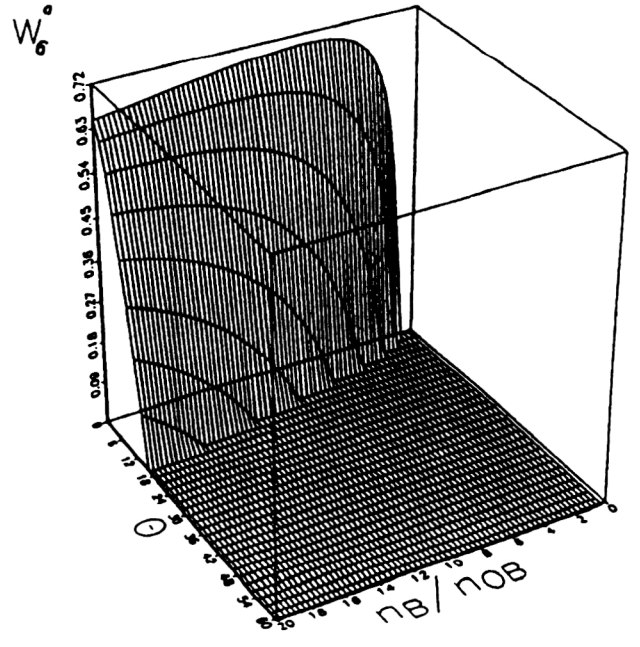

FIG. 46. The probability of condensed six-quark clusters.

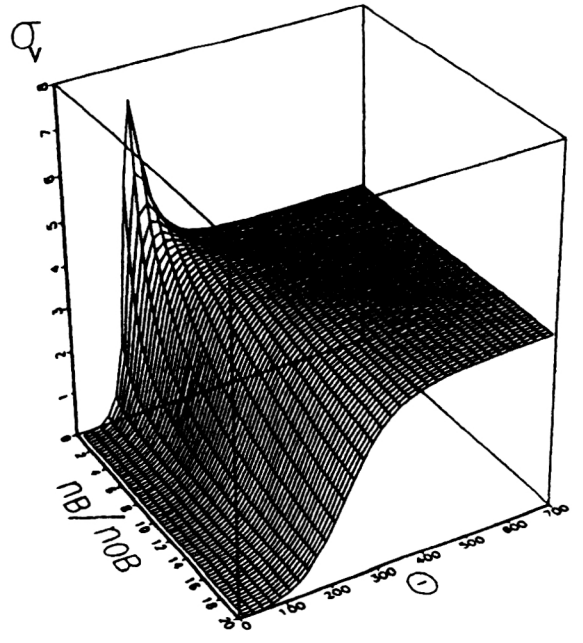

FIG. 48. Reduced specific heat.

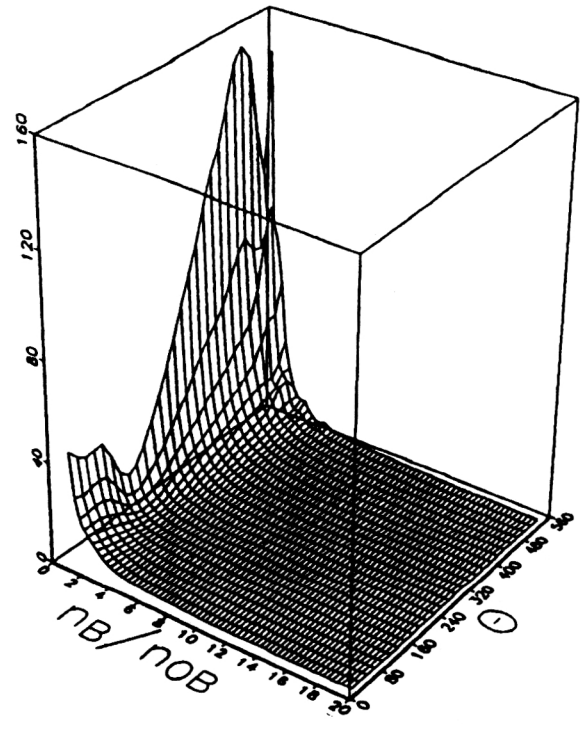

FIG. 49. Dimensionless compressibility coefficient.

hadron–plasma state, rules out those predictions that have been based on a sharp first-order phase transition. This concerns the interpretation of signals of the quark–gluon plasma in heavy-ion collisions[8–14,159] and the hadronization scenario related to the evolution of the early universe after the Big Bang.[4] The quantitative predictions of our approach can be

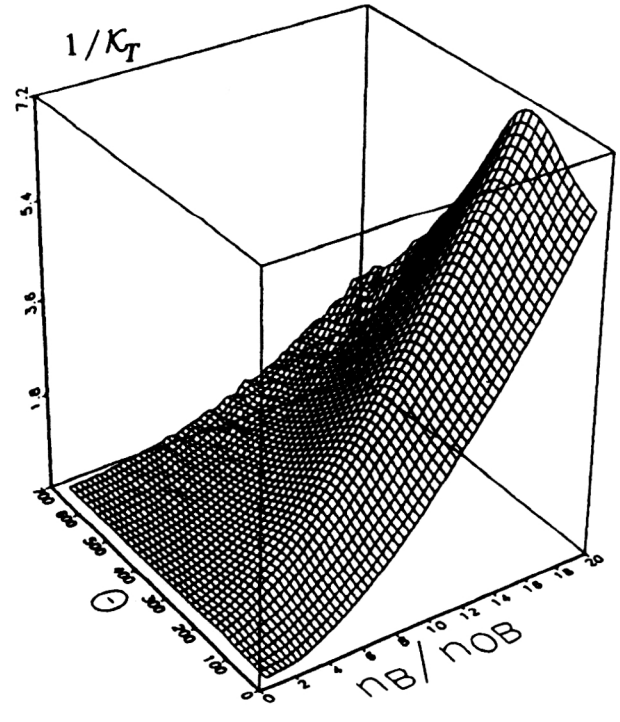

FIG. 50. Dimensionless compression modulus as a function of temperature and baryon density.

improved in several ways, for instance, by including more kinds of particles or by invoking more elaborate interaction potentials.[160] However, we hope that qualitatively the picture will remain the same.

We are greatly indebted to A. M. Baldin for stimulating one of the authors (V.I.Y.) by the problem considered, for constant support, and for much valuable advice. We acknowledge, with pleasure and gratitude, a number of fruitful discussions with our colleagues from the Relativistic Nuclear Physics Group at Dubna, especially V. V. Burov, V. K. Lukyanov, and A. I. Titov. We appreciate the help of our co-authors collaborating with us at different stages of our work.

[1] A. M. Baldin, Sov. J. Part. Nucl. **8**, 175 (1977).
[2] E. V. Shuryak, Phys. Rep. **61**, 71 (1980).
[3] D. J. Gross, R. D. Pisarski, and L. G. Yaffe, Rev. Mod. Phys. **53**, 43 (1981).
[4] J. Cleymans, R. Gavai, and E. Suhonen, Phys. Rep. **130**, 217 (1986).
[5] L. McLerran, Rev. Mod. Phys. **58**, 1021 (1986).
[6] B. Müller, Rep. Prog. Phys. **58**, 611 (1995).
[7] H. Reeves, Phys. Rep. **201**, 335 (1991).
[8] F. Halzen, Contemp. Phys. **24**, 591 (1983).
[9] L. P. Csernai and J. I. Kapusta, Phys. Rep. **131**, 233 (1986).
[10] R. Stöck, Phys. Rep. **135**, 260 (1986).
[11] H. Stöcker and W. Greiner, Phys. Rep. **137**, 277 (1986).
[12] R. Clare and D. Strottman, Phys. Rep. **141**, 177 (1986).
[13] P. Koch, B. Müller, and J. Rafelski, Phys. Rep. **142**, 167 (1986).
[14] K. Geiger, Phys. Rep. **258**, 237 (1995).
[15] V. I. Yukalov, Phys. Rep. **208**, 395 (1991).
[16] P. S. Isaev, *Quantum Electrodynamics at High Energies* (AIP, New York, 1989).
[17] G. Sterman *et al.*, Rev. Mod. Phys. **67**, 157 (1995).
[18] E. Fermi, Prog. Theor. Phys. **5**, 570 (1950).
[19] R. Hagedorn, Nuovo Cimento Suppl. **3**, 147 (1965).
[20] R. Hagedorn, I. Montvay, and J. Rafelski, in *Hadronic Matter at Extreme Energy Density*, edited by N. Cabibbo and L. Sertorio (Plenum, New York, 1980), p. 49.
[21] J. C. Collins and M. J. Perry, Phys. Rev. Lett. **34**, 1353 (1975).
[22] C. W. Wong, Phys. Rep. **136**, 1 (1986).
[23] J. Baacke, Acta Phys. Pol. B **8**, 625 (1977).
[24] D. Stauffer, *Introduction to Percolation Theory* (Taylor and Francis, London, 1985).
[25] M. I. Gorenstein, S. A. Lipskikh, and G. M. Zinovjev, Z. Phys. C **18**, 13 (1984).
[26] E. H. Lieb, Bull. Am. Math. Soc. **22**, 1 (1990).
[27] A. Jackson and T. Wetting, Phys. Rep. **237**, 325 (1994).
[28] J. W. Negele, Rev. Mod. Phys. **54**, 913 (1982).
[29] E. V. Shuryak, Phys. Rep. **115**, 151 (1984).
[30] V. M. Emelyanov, Y. P. Nikitin, and A. V. Vanyashin, Fortschr. Phys. **38**, 1 (1990).
[31] C. G. Källman, Phys. Lett. B **134**, 363 (1984).
[32] I. V. Moskalenko and D. E. Kharzeev, Yad. Fiz. **48**, 1122 (1988) [Sov. J. Nucl. Phys. **48**, 713 (1988)].
[33] V. I. Yukalov, Int. J. Mod. Phys. B **3**, 1691 (1989).
[34] V. I. Yukalov, Physica A **167**, 833 (1990).
[35] V. I. Yukalov, Phys. Rev. A **42**, 3324 (1990).
[36] V. I. Yukalov, J. Math. Phys. **32**, 1235 (1991).
[37] V. I. Yukalov, J. Math. Phys. **33**, 3994 (1992).
[38] V. I. Yukalov and E. P. Yukalova, Nuovo Cimento B **108**, 1017 (1993).
[39] V. I. Yukalov and E. P. Yukalova, Physica A **206**, 553 (1994).
[40] V. I. Yukalov and E. P. Yukalova, Laser Phys. **5**, 154 (1995).
[41] B. Godwal, S. Sikha and R. Chidambaram, Phys. Rep. **102**, 121 (1983).
[42] J. B. Kogut, Phys. Rep. **67**, 67 (1980).
[43] J. Engels, F. Karsch, H. Satz, and I. Montvay, Nucl. Phys. B **205**, 545 (1982).
[44] F. R. Brown, Nucl. Phys. B Proc. Suppl. **9**, 311 (1989).
[45] Y. Deng, Nucl. Phys. B Proc. Suppl. **9**, 334 (1989).
[46] J. Engels, J. Fingberg, and M. Weber, Nucl. Phys. B Proc. Suppl. **9**, 378 (1989).
[47] B. Peterson, Nucl. Phys. A **525**, 237 (1991).
[48] S. Gottlieb, Nucl. Phys. B Proc. Suppl. **20**, 247 (1991).

[49] A. Vaccarino, Nucl. Phys. B Proc. Suppl. **20**, 263 (1991).
[50] J. Engels, Nucl. Phys. B Proc. Suppl. **20**, 325 (1991).
[51] F. Karsch and E. Laermann, Rep. Prog. Phys. **56**, 1347 (1993).
[52] J. Engels, F. Karsch, and K. Redlich, Nucl. Phys. B **435**, 295 (1995).
[53] D. H. Rischke, Nucl. Phys. A **583**, 663 (1995).
[54] V. I. Yukalov and A. S. Shumovsky, *Lectures on Phase Transitions* (World Scientific, Singapore, 1990).
[55] E. V. Shuryak, Rev. Mod. Phys. **65**, 1 (1993).
[56] C. DeTar, Phys. Rev. D **32**, 276 (1985).
[57] T. A. DeGrand and C. E. DeTar, Phys. Rev. D **34**, 2469 (1986).
[58] T. A. DeGrand and C. E. DeTar, Phys. Rev. D **35**, 742 (1987).
[59] C. E. DeTar and J. B. Kogut, Phys. Rev. D **36**, 2828 (1987).
[60] C. DeTar, Phys. Rev. D **37**, 2328 (1988).
[61] T. Hatsuda and T. Kunihiro, Phys. Lett. B **145**, 7 (1984).
[62] T. Hatsuda and T. Kunihiro, Phys. Rev. Lett. **55**, 158 (1985).
[63] T. Hatsuda and T. Kunihiro, Prog. Theor. Phys. **74**, 765 (1985).
[64] T. Hatsuda and T. Kunihiro, Phys. Lett. B **185**, 304 (1987).
[65] B. I. Ivlev and N. B. Kopnin, Usp. Fiz. Nauk **142**, 435 (1984) [Sov. Phys. Usp. **27**, 206 (1984)].
[66] G. E. Volovik, Usp. Fiz. Nauk **143**, 73 (1984) [Sov. Phys. Usp. **27**, 363 (1984)].
[67] T. Schäfer, and E. V. Shuryak, Phys. Lett. B **356**, 147 (1995).
[68] C. Adami and G. E. Brown, Phys. Rep. **234**, 1 (1993).
[69] J. B. Kogut, D. K. Sinclair, and K. C. Wang, Phys. Lett. B **263**, 101 (1991).
[70] J. Clark, J. Cleymans, and J. Rafelski, Phys. Rev. C **33**, 703 (1986).
[71] P. Z. Bi and Z. P. Shi, Phys. Rev. C **38**, 1069 (1988).
[72] A. Kumar, H. Krishnamurthy, and E. Gopal, Phys. Rep. **98**, 58 (1983).
[73] F. De Leeuw, R. Van den Doel, and U. Enz, Rep. Prog. Phys. **43**, 689 (1980).
[74] G. G. Bunatyan, Yad. Fiz. **43**, 294 (1986) [Sov. J. Nucl. Phys. **43**, 188 (1986)].
[75] G. G. Bunatyan, Yad. Fiz. **51**, 1243 (1990) [Sov. J. Nucl. Phys. **51**, 790 (1990)].
[76] C. J. Horowitz, Phys. Lett. B **162**, 25 (1985).
[77] M. Oka and C. J. Horowitz, Phys. Rev. D **31**, 2773 (1985).
[78] P. J. S. Watson, Nucl. Phys. A **494**, 543 (1989).
[79] C. J. Horowitz and J. Piekarewicz, Phys. Rev. C **44**, 2753 (1991).
[80] C. J. Horowitz and J. Piekarewicz, Nucl. Phys. A **536**, 669 (1992).
[81] S. Gardner, C. J. Horowitz, and J. Piekarewicz, Phys. Rev. C **50**, 1137 (1994).
[82] M. Nzar and P. Hoodbhoy, Phys. Rev. C **42**, 1778 (1990).
[83] W. Melendez and C. J. Horowitz, Comput. Phys. **9**, 450 (1995).
[84] J. E. Enderby and G. W. Neilson, Adv. Phys. **29**, 323 (1980).
[85] J. E. Enderby, Contemp. Phys. **24**, 561 (1983).
[86] V. I. Yukalov, Theor. Math. Phys. **17**, 1244 (1973).
[87] V. I. Yukalov, in *Problems in Quantum Field Theory*, edited by N. N. Bogolubov (JINR, Dubna, 1987), p. 62.
[88] V. I. Yukalov, Int. J. Theor. Phys. **28**, 1237 (1989).
[89] V. I. Yukalov, Nuovo Cimento A **103**, 1577 (1990).
[90] D. Blaschke, F. Reinholz, G. Röpke, and D. Kremp, Phys. Lett. B **151**, 439 (1985).
[91] G. Röpke, D. Blaschke, and H. Schulz, Phys. Rev. D **34**, 3499 (1986).
[92] G. Röpke, D. Blaschke, and H. Schulz, Phys. Lett. B **202**, 479 (1988).
[93] G. Röpke, D. Blaschke, and H. Schulz, Phys. Rev. D **38**, 3589 (1988).
[94] G. Röpke, L. Münchow, and H. Schulz, Nucl. Phys. A **379**, 536 (1982).
[95] G. Röpke, M. Schmidt, L. Münchow, and H. Schulz, Nucl. Phys. A **399**, 587 (1983).
[96] H. R. Glyde and G. H. Keech, Ann. Phys. (N.Y.) **127**, 330 (1980).
[97] J. B. Boyce and B. A. Huberman, Phys. Rep. **51**, 189 (1979).
[98] H. S. Chen, Rep. Prog. Phys. **43**, 353 (1980).
[99] N. K. Glendenning, Phys. Rev. D **46**, 1274 (1992).
[100] V. V. Burov, V. K. Lukyanov, and A. I. Titov, Fiz. Élem. Chastits At. Yadra **15**, 1249 (1984) [Sov. J. Part. Nucl. **15**, 558 (1984)].
[101] B. L. Bakker and I. M. Narodetskii, Adv. Nucl. Phys. **21**, 1 (1994).
[102] A. M. Baldin, R. G. Nazmitdinov, A. V. Chizhov, A. S. Shumovsky, and V. I. Yukalov, Sov. Phys. Dokl. **29**, 952 (1984).
[103] A. M. Baldin, R. G. Nazmitdinov, A. V. Chizhov, A. S. Shumovsky, and V. I. Yukalov, in *Multiquark Interactions and Quantum Chromodynamics*, edited by A. M. Baldin (JINR, Dubna, 1984), p. 531.
[104] A. V. Chizhov, R. G. Nazmitdinov, A. S. Shumovsky, and V. I. Yukalov, JINR Rapid Commun. No. 7, 45 (1985).
[105] A. M. Baldin, A. S. Shumovsky, and V. I. Yukalov, Phys. Many-Part. Syst. **10**, 10 (1986).
[106] A. V. Chizhov, R. G. Nazmitdinov, A. S. Shumovsky, and V. I. Yukalov, Nucl. Phys. A **449**, 660 (1986).
[107] Y. A. Troian, A. V. Nikitin, V. N. Pechenov, Y. D. Beznogikh, A. G. Doroshenko, and A. P. Tsarenkov, Yad. Fiz. **54**, 1301 (1991) [Sov. J. Nucl. Phys. **54**, 792 (1991)].
[108] R. L. Jaffe, Phys. Rev. Lett. **38**, 195 (1977).
[109] V. A. Matveev and P. Sorba, Nuovo Cimento A **45**, 257 (1978).
[110] A. A. Shanenko, A. S. Shumovsky, and V. I. Yukalov, Int. J. Mod. Phys. A **4**, 2235 (1989).
[111] J. P. Blaizot, Phys. Rep. **64**, 171 (1980).
[112] V. I. Kukulin, and V. N. Pomerantsev, Prog. Theor. Phys. **88**, 159 (1992).
[113] R. Mchleidt, K. Holinde, and C. Elster, Phys. Rep. **149**, 1 (1987).
[114] V. I. Yukalov, Rep. Inst. Sci. Tech. Inf. No. 3684, 1 (1975).
[115] A. A. Shanenko and V. I. Yukalov, in *Relativistic Nuclear Physics and Quantum Chromodynamics*, edited by A. M. Baldin (JINR, Dubna, 1988), Vol. 1, p. 445.
[116] E. P. Kadantseva, A. A. Shanenko, and V. I. Yukalov, in *Selected Topics in Statistical Mechanics*, edited by A. A. Logunov (World Scientific, Singapore, 1990), p. 412.
[117] E. P. Kadantseva, A. A. Shanenko, and V. I. Yukalov, Phys. Lett. B **255**, 427 (1991).
[118] E. P. Kadantseva, A. A. Shanenko, and V. I. Yukalov, in *Relativistic Nuclear Physics and Quantum Chromodynamics*, edited by A. M. Baldin, V. V. Burov, and L. P. Kaptari (World Scientific, Singapore, 1991), p. 602.
[119] V. I. Yukalov, E. P. Kadantseva, and A. A. Shanenko, Nuovo Cimento A **105**, 371 (1992).
[120] J. P. Vary, Nucl. Phys. A **418**, 195 (1984).
[121] C. Bernard *et al.*, Phys. Rev. Lett. **68**, 2125 (1992).
[122] V. I. Yukalov, E. P. Yukalova, and A. A. Shanenko, in *Symmetry Methods in Physics*, edited by A. N. Sissakian, G. S. Pogosyan, and S. I. Vinitsky (JINR, Dubna, 1994), Vol. 2, p. 592.
[123] E. P. Kadantseva, A. A. Shanenko, and V. I. Yukalov, in *Standard Model and Beyond*, edited by S. Dubnicka, D. Ebert, and A. Sazonov (World Scientific, Singapore, 1991), p. 201.
[124] E. P. Kadantseva, A. A. Shanenko, and V. I. Yukalov, Sov. J. Nucl. Phys. **55**, 435 (1992).
[125] A. A. Shanenko, E. P. Yukalova, and V. I. Yukalov, Hadronic J. **16**, 1 (1993).
[126] K. L. Au, D. Morgan, and M. R. Pennington, Phys. Lett. B **167**, 229 (1986).
[127] M. Boutemer and J. Peigneux, Nucl. Phys. B Proc. Suppl. **21**, 159 (1991).
[128] J. Kogut, D. Sinclair, and L. Susskind, Nucl. Phys. B **114**, 199 (1976).
[129] B. Berg and A. Billoire, Nucl. Phys. B **221**, 109 (1983).
[130] R. Gupta, A. Patel, C. Baillie, G. Kilcup, and S. Sharpe, Phys. Rev. D **43**, 2301 (1991).
[131] H. Fritzsch and P. Minkowski, Nuovo Cimento A **30**, 393 (1975).
[132] R. Jaffe and K. Johnson, Phys. Lett. B **60**, 201 (1975).
[133] J. Donoghue, K. Johnson, and B. Li, Phys. Lett. B **99**, 416 (1981).
[134] J. Engels, F. Karsch, I. Monvay, and H. Satz, Phys. Lett. B **101**, 89 (1981).
[135] J. Engels, J. Finberg, K. Redlich, H. Satz, and M. Weber, Z. Phys. C **42**, 341 (1989).
[136] F. Brown, N. Christ, Y. Deng, M. Gao, and T. Woch, Phys. Rev. Lett. **61**, 2058 (1988).
[137] T. Çelik, J. Engels, and H. Satz, Nucl. Phys. B **256**, 670 (1985).
[138] D. Ter Haar, *Elements of Statistical Mechanics* (Rinehart, New York, 1954).
[139] J. Zimányi, B. Lukács, P. Lévai, J. Bondorf, and N. Balazs, Nucl. Phys. A **484**, 647 (1988).
[140] D. H. Rischke, B. L. Friman, H. Stöcker, and W. Greiner, J. Phys. G **14**, 191 (1988).
[141] A. A. Shanenko, E. P. Yukalova, and V. I. Yukalov, Physica A **197**, 629 (1993).
[142] A. A. Shanenko, E. P. Yukalova, and V. I. Yukalov, in *Symmetry and Structural Properties of Condensed Matter*, edited by W. Florek, D. Lipinski, and T. Lulek (World Scientific, Singapore, 1993), p. 237.
[143] E. Eichten, K. Gottfried, T. Kinoshita, K. Lane, and T. Yan, Phys. Rev. D **17**, 3090 (1978).
[144] E. Eichten, K. Gottfried, T. Kinoshita, K. Lane, and T. Yan, Phys. Rev. D **21**, 203 (1980).
[145] Y. A. Simonov, Yad. Fiz. **54**, 192 (1991) [Sov. J. Nucl. Phys. **54**, 115 (1991)].
[146] H. Q. Ding, Int. J. Mod. Phys. C **2**, 637 (1991).

[147] S. Mukherjee, R. Nag, S. Sanyal, T. Morii, J. Morishita, and M. Tsuge, Phys. Rep. **231**, 201 (1993).
[148] A. A. Shanenko, E. P. Yukalova, and V. I. Yukalov, Phys. At. Nucl. **56**, 372 (1993).
[149] A. A. Shanenko, E. P. Yukalova, and V. I. Yukalov, Nuovo Cimento A **106**, 1269 (1993).
[150] A. A. Shanenko, E. P. Yukalova, and V. I. Yukalov, in *Proceedings of the Workshop on Soft Physics*, edited by G. Bugrij, L. Jenkovsky, and E. Martynov (Ukrainian Academy of Sciences, Kiev, 1993), p. 111.
[151] A. A. Shanenko, E. P. Yukalova, and V. I. Yukalov, in *Relativistic Nuclear Physics and Quantum Chromodynamics*, edited by A. M. Baldin and V. V. Burov (JINR, Dubna, 1994), p. 191.
[152] F. R. Brown *et al.*, Phys. Rev. Lett. **65**, 2491 (1990).
[153] T. H. Barron, J. G. Collins, and G. K. White, Adv. Phys. **29**, 609 (1980).
[154] A. A. Shanenko, E. P. Yukalova, and V. I. Yukalov, in *Hadrons and Nuclei from Quantum Chromodynamics*, edited by K. Fujii, Y. Akaishi, and B. Reznik (World Scientific, Singapore, 1994), p. 109.
[155] A. A. Shanenko, E. P. Yukalova, and V. I. Yukalov, Phys. Dokl. **40**, 291 (1995).
[156] A. A. Shanenko, E. P. Yukalova, and V. I. Yukalov, Phys. At. Nucl. **58**, 335 (1995).
[157] A. A. Shanenko, E. P. Yukalova, and V. I. Yukalov, JINR Rapid Commun. No. 69, 19 (1995).
[158] L. Mornas and U. Ornik, Nucl. Phys. A **587**, 828 (1995).
[159] C. P. Singh, Phys. Rep. **236**, 147 (1993).
[160] M. Hjorth-Jensen, T. Kuo, and E. Osnes, Phys. Rep. **261**, 125 (1995).

This article was published in English in the original Russian journal. It is reproduced here with the stylistic changes by the Translations Editor.